Passenger kinematics in braking, lane change and oblique driving maneuvers

Philipp Huber, Stefan Kirschbichler, Adrian Prüggler, Thomas Steidl

Abstract A series of vehicle-based driving maneuvers was performed, where occupants in the passenger position were subjected to emergency braking maneuvers at 12 km/h and 50 km/h, lane change maneuvers to the left and the right and combined maneuvers, where a combination of lateral and frontal accelerations occurred. A comprehensive collection of vehicle and occupant kinematic corridors based on results from 6 female (mass: 63.0±10.4 kg, height: 169.0±4.1 cm, age: 31.5±9.3 y) and 19 male (mass: 77.8±8.4 kg, height: 178.2±5.0 cm, age: 28.2±3.8 y) subjects are presented.

Asymmetries in the response as well as the detailed kinematics are discussed for selected load cases, before results of various maneuvers are related to each other.

Keywords Combined maneuver, emergency braking, lane change maneuver, low g vehicle test, occupant kinematics

I. INTRODUCTION

In order to further improve vehicle safety and work towards the European Commission's target of reducing the number of fatalities caused by traffic accidents by half in the decade between 2011 and 2020 [1] and finally arriving at the "vision zero" [2] promising path of active and integrated safety systems. Such systems need robust development tools, which are currently being devised. In contrast to the crash phase, where the occupant's motion is predominantly determined by the body's inertia and material behavior, in the pre-crash phase also muscle-induced movement has a significant influence on the kinematics. Active human body models are numerical simulation tools to describe this pre-crash phase including active muscle contributions.

The human kinematic response in pre-crash type loading conditions, i.e. acceleration in the order of 1 g, has been studied over the last decade, where two main classes of studies can be found in the literature, sled-based studies and vehicle-based tests. In a series of publications [3-5] the biomechanical response of male and female subjects was studied during low-speed sled tests in both frontal and lateral directions, reporting a considerable effect of the individual muscle contribution to the subject's motion. In a follow-up study [6] the effect of a motorized seat belt was shown to reduce the subjects' forward motion. In [7] and [8] volunteers, post mortem human surrogates and a Hybrid III 50th percentile male anthropomorphic test device were subjected to sled accelerations with peak values of 2.5 g and 5 g, revealing qualitatively different biomechanical responses of the groups. Also the active bracing effect was studied for human subjects, which was found to significantly reduce the upper body forward excursion. In [9] lateral evasive maneuvers with a peak acceleration of 0.5 g were performed, where 10 subjects were restrained using a four-point belt and both relaxed and braced conditions were reported.

Vehicle-based studies of manual as well as autonomous braking of male and female subjects were performed in [10-12], where also driver and passenger behavior was studied.

The work in [13-14] can be considered as precursor to the present paper, where vehicle based emergency braking, lane change and combined maneuvers are presented. For a lap-belt and rigid seat configuration between 20 and 22 subjects were reported, while for a combination of a three-point belt and a seat with cushions and lateral support structures a preliminary subset of results was presented (emergency braking 12 km/h unaware: 4 female, 10 male; first repetition: 3 female, 6 male; 50 km/h: 4 female, 6 male; lane change to the left: 3 female, 2 male; right: 2 female, 2 male; combined maneuver to the left and right: 1 female, 3 male).

From the literature no results for oblique loading directions, i.e. maneuvers where subjects are accelerated in frontal and lateral directions, were found, neither for sled-based tests, nor for vehicle-based test. Also typical studies concentrated on a loading direction, where either loading conditions (e.g. peak acceleration) or subject

P. Huber is Lead Researcher, A. Prüggler and T. Steidl are Junior Researchers at Virtual Vehicle Research Center, Graz, Austria. S. Kirschbichler is Junior Researcher at the Vehicle Safety Institute at Graz University of Technology, Austria.

preparation (e.g. braced or tensed, driver or passenger) were varied. In this study as well as in [13-14] detailed 3D occupant kinematics of a large number of subjects is presented for five different loading directions in the first part of the paper. In the second part of the paper the occupant kinematics between the different load cases are addressed and also inter- and intra-subject variability are discussed.

II. METHODS

A. Vehicle and maneuvers

On a closed test track three main types of maneuvers, emergency braking, lane change and combination of braking and steering were performed with subjects in the passenger position. A Mercedes-Benz S-500 (type: W221, width: 1.78 m, length: 5.23 m, wheelbase: 3.17 m, left-hand drive, see Fig. 2) was used as test vehicle.

In the emergency braking maneuver (initial velocities of 12 km/h and 50 km/h, referred to as maneuvers *Brake12_01* or *Brake12_02* and *Brake50_01* respectively, where the suffix *01* indicates that it was the first maneuver of this kind for the subject and the suffix *02* indicates the first repetition of the maneuver) the driver pressed the brake pedal at maximum effort, leading to a support by the vehicle's brake-assistant system. In the lane change maneuver to the right (*LaneRight50*) the driver initiated the maneuver by turning the steering wheel to the right by approximately 200° within typically 0.5 s followed by a counter steering action of around 360° within 0.7 s and a return movement to the neutral position. In the lane change maneuver to the left (*LaneLeft50*) similar actions, in the opposite direction, were performed. In both maneuvers the initial velocity was 50 km/h. In the combined maneuver the driver turned the steering wheel by approximately 220° within 0.6 s while simultaneously pressing the brake pedal at sufficient effort to activate the brake assistant system (*CombinedLeft50* and *CombinedRight50*).

All test sequences started with an emergency braking maneuver at 12 km/h in order to allow a comparison to results in [13], where unaware subjects were tested using a lap belt only. All subsequent maneuvers (*Brake12_02*, *Brake50_01, LaneRight50, LaneLeft50*, *CombinedLeft50* and *CombinedRight50*) were performed in random order.

The vehicle's velocity (sample rate: 10 Hz), acceleration in frontal and lateral directions (50 Hz), steering wheel angel and associated angular velocity (100 Hz), yaw rate and brake pedal activation state (50 Hz) were recorded from the CAN Bus using a Dewetron Dewe 5000 system.

For braking and combined maneuvers the brake pedal state, indicating the initial brake pedal contact, was used to define the start of the maneuver referred to as t=0. In the lane change maneuvers a threshold value for the steering wheel angle of 20° was defined. At the time instance, where the threshold value was reached, the steering wheel angular velocity was used to extrapolate to the neutral steering wheel position. The corresponding time instance was defined as t=0 (see also [15]).

B. Subjects

Results from 6 female (mass: 63.0±10.4 kg, height: 169.0±4.1 cm, age: 31.5±9.3 y) and 19 male (mass: 77.8±8.4 kg, height: 178.2±5.0 cm, age: 28.2±3.8 y) subjects are presented in the study. All subjects gave written informed consent after written and verbal explanation of the test procedure. No specifics about the driving maneuvers were given other than that only maneuvers that can be encountered in normal driving were done. The subjects held a valid driving license for the operation of a passenger vehicle. Subjects were instructed to relax and sit in a comfortable passenger position. The test procedure was reviewed and approved by the ethics committee at the Medical University of Graz. Some trials had to be excluded due to bad data quality. Therefore the anthropometric properties for the subset of valid trials per maneuver are presented in Table 1.

TABLE I
PARAMETERS OF THE MANEUVER AND SUBJECT PROPERTIES

maneuver	velocity [km/h]	#subjects	#male	#female	height [cm] mean ±std.dev.	weight [kg] mean ±std.dev.
Brake12_01	12	25	19	6	176.0±6.1	74.7±10.8
Brake12_02	12	25	19	6	176.0±6.1	74.7±10.8
Brake50_01	50	23	17	6	175.7±6.4	73.9±10.4
LaneLeft50	50	21	16	5	175.8±6.3	73.7±11.5

LaneRight50	50	21	16	5	175.7±6.1	73.7±11.5
CombinedLeft50	50	21	15	6	175.9±7.1	74.1±12.5
CombinedRight50	50	20	17	3	177.3±5.8	76.8±9.7

C. Seat and belt

A modified seat (Fig. 2), where the original seat's foam cushions were removed and replaced by wooden plates was used in the tests. Lateral support structures were added, where the geometry was oriented around the geometry of the original seat (angle lateral support: 120°, distance between left and right piece: 314 mm, angle of back rest: 104°). A layer of foam (thickness: 40 mm) was applied to the seat surface and back rest as well as the lateral support structures. All foam parts were then covered in artificial leather and a layer of infrared-absorbing material to reduce reflections that may compromise the motion tracking camera's recording quality. Since the original seat has a complex geometry and foam layup this setup was chosen to allow a more straight-forward translation into a numerical simulation environment. The standard three-point belt was used with the pre-tensioner disabled.

D. Occupant kinematics

All subjects wore a skin-tight suit to minimize soft tissue artifacts and a set of retro-reflective markers was applied to the suit and hat. Eight Vicon M2 near-infrared motion tracking cameras recorded occupant kinematic data at a frame rate of 100 Hz and data was processed in a Vicon V612 data station. For the system to work properly the windshield had to be removed and a modified passenger door without window and with material removed from the lower part of the door had to be used. In order to compensate for camera vibrations in the moving vehicle a correction algorithm was applied [16]. Thereafter the standard process of 3D reconstruction and trajectory labeling was followed. Missing segments in the trajectory data, e.g. due to marker occlusions, were interpolated using a purpose-built gap-filling procedure based on a rigid body assumption for markers on certain body segment.

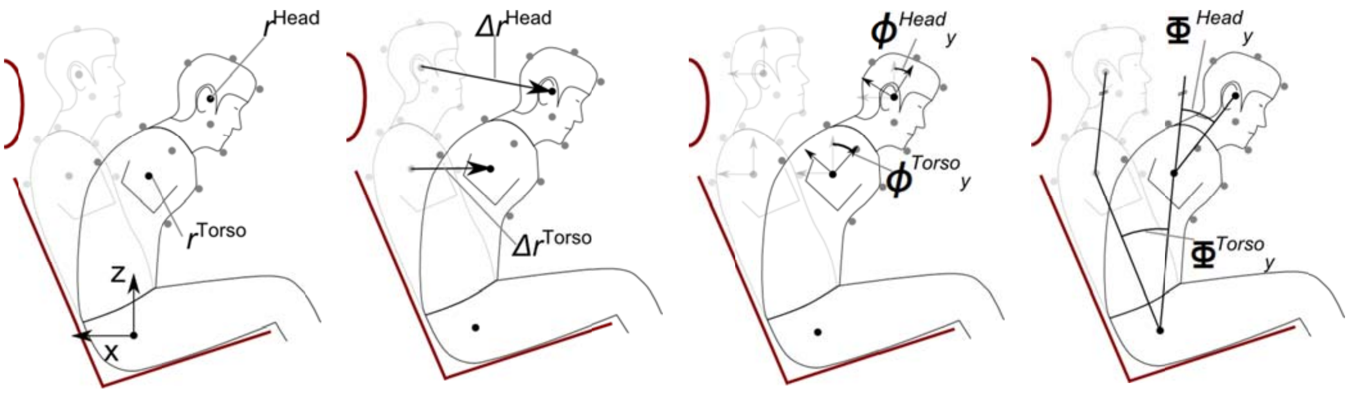

(a) (b) (c) (d)

Fig. 1: Characteristic kinematic quantities for head and torso motion. The light grey pose refers to the initial pose of the, while the dark pose depicts the situation during the maneuver. (a) location of head and torso centroids r^{Head} and r^{Torso} computed from corresponding segment markers (b) relative displacement of the centroid of head and torso markers Δr^{Head} and Δr^{Torso} with respect to the location at t=0 (c) head and torso segment orientation ϕ^{Head} and ϕ^{Torso} (d) head and torso centroid angle Φ^{Head} and Φ^{Torso}.

In order to derive characteristic kinematic quantities for head and torso 11 markers on the head (bilateral: forehead, back of the head, ear, cheek bone; central: top of head, C1, chin; referred to as head segment markers) and 12 markers on the torso (bilateral acromion, pectoralis, clavicle, scapula; central: C7, T1, T10, sternum; referred to as torso segment markers) were used to compute centroid trajectories, which lie at ear and T5 level for the head and torso. The coordinates of these centroids were denoted $r^{Head|Torso}_{x|y|z}$ and given in a Cartesian coordinate system, where the origin was located at the seat's H-point. The x-axis was oriented to the back of the vehicle and the y-axis points to the right of the vehicle (Fig. 1a). The relative displacement of the centroid of head and torso markers with respect to the location at t=0 were denoted $\Delta r^{Head|Torso}_{x|y|z}$ (Fig. 1b). Due to the choice of coordinate system $\Delta r_x < 0$ refers to forward movement and $\Delta r_y > 0$ to a movement to the left.

From the head and torso segment markers also an orientation relative to the configuration at t=0 was computed. The corresponding rotation angles around the x-, y- and z-axes were denoted $\phi^{Head|Torso}_{x|y|z}$ and referred to as segment orientations (Fig. 1c). Here ϕ_x>0 refers to rotation towards the center of the vehicle and ϕ_y<0 to a forward rotation.

If there is no bending of lumbar and thoracical spine, i.e. the whole torso behaves as rigid body, there is a direct correspondence between Δr and ϕ. In contrast flection in e.g. the lower part of the lumbar spine and extention in the upper part of the lumbar spine could lead to a forward movement of the torso centroid, while there is no change in upper torso orientation. Therefore an orientation matrix between the vector from the H-point to r^{Torso} and the corresponding vector in the initial position t=0 was computed and the rotation angle around x-, y- and z-axes were then denoted as $\Phi^{Torso}_{x|y|z}$ (Fig. 1d). The analogous procedure using the vector r^{Head}-r^{Torso} was performed to obtain $\Phi^{Head}_{x|y|z}$. Note that due to the definition positive values of Φ relate to negative values in ϕ and vice versa. Comparing e.g. the two angles ϕ^{Torso}_y and $-\Phi^{Torso}_y$ allows to estimate lumbar spine bending, where the case $\phi^{Torso}_y = -\Phi^{Torso}_y$ indicates no effective bending.

No distinct smoothing procedure was employed, except for the inherent low-pass filter properties associated with position and orientation estimation described above.

For each of the four quantities r, Δr, ϕ and Φ, kinematic corridors were derived. In each recorded time instance the median, 0.16^{th} and 0.84^{th} quantile of the kinematic quantity in consideration was computed and displayed against time. These values were chosen such that 68% of the data lie within the corridor, which corresponds to a width of twice the standard deviation in case of an underlying normal distribution. Choosing median and specific quantile curves has the benefit of preserving some information about the skewness of the data.

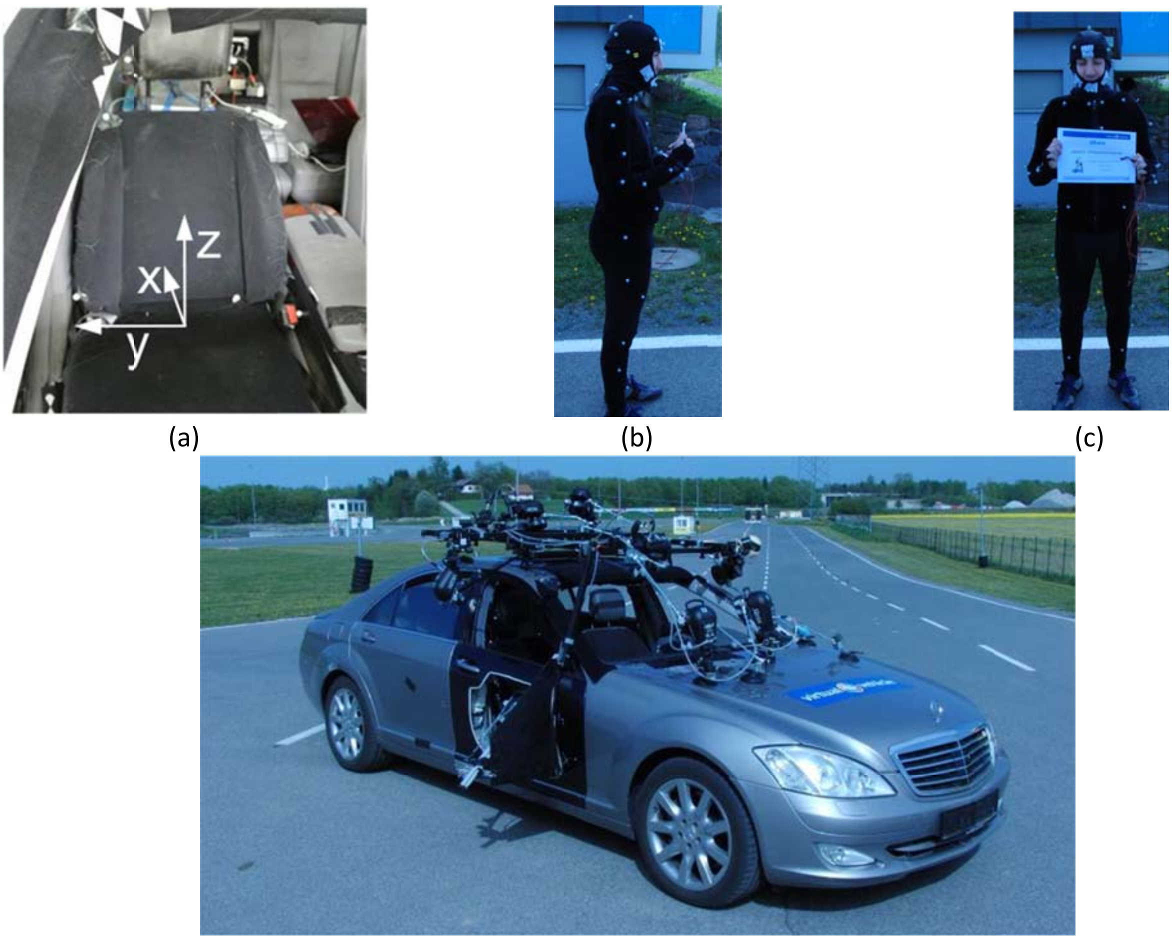

(a) (b) (c)

(d)

Fig. 2: Setup of vehicle and subjects. A modified seat (a) was used in the vehicle (d). Passenger window and windshield were removed, and a Vicon eight camera infrared-based motion capturing system was mounted on the vehicle. Subjects wore a skin-tight suit and retro-reflective markers were applied (b) and (c).

For further analysis the maximum excursions of Δr_x and Δr_y within the interval $0 \leq t \leq 0.6$ s for 12 km/h braking maneuvers and $0 \leq t \leq 1.2$ s for the remaining maneuvers was used. For maneuvers to the right the minimal value of Δr_y corresponds to the maximum initial excursion, while in the maneuvers to the left the maximum value was chosen. In order to compare excursions in maneuvers to the left and right these peak values were used in an analysis of variation (ANOVA).

III. RESULTS

In the description of the maneuvers the following approach was taken. First vehicle and occupant kinematics of emergency braking, lane change and combined maneuvers are presented separately. A full set of kinematic curves is given in the appendix, while selected plots are discussed in the main part of the paper. Thereafter the maximum excursions during emergency braking, lane change and combined maneuvers are discussed and related to each other and finally inter- and intra-subject variability is addressed.

A. Emergency braking

Emergency braking maneuvers were performed twice at a velocity of 12 km/h and once at 50 km/h (referred to as *Brake12_01*, *Brake12_02* and *Brake50_01* in the remainder of this work). In Fig. 3 velocity and frontal acceleration are presented.

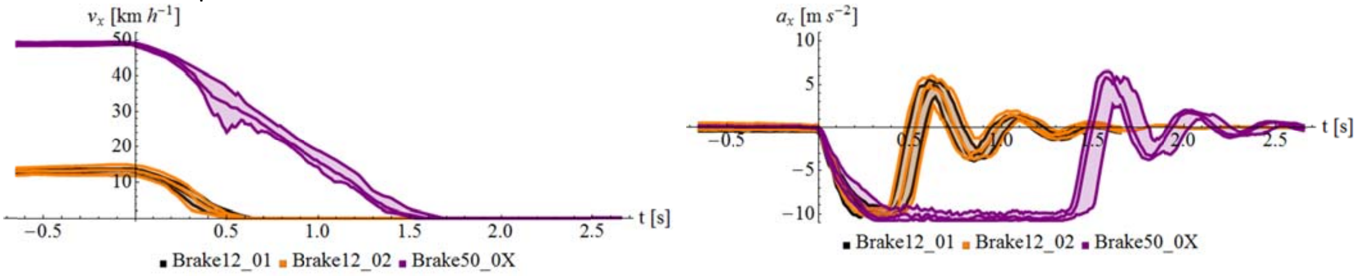

Fig. 3: Corridors for velocity v_x (left) and frontal acceleration a_x (right) for the three emergency braking maneuvers are displayed against time. Both values are recorded from CAN-bus data. Note that there are some artifacts in the velocity plots for *Brake50_01* occurring at around t=0.5 s, which are likely due to a locking of the wheels, as the associated accelerations do not show such behavior.

The full set of results for occupant kinematics for emergency maneuvers is collected in the appendix (Fig. 15-Fig. 18). The dominant movement for all three maneuvers occurs in the sagittal plane and the associated quantities are displayed in Fig. 16, while in Fig. 4 only the displacement in frontal direction is presented. The occupant movement can be divided into two main phases, a forward movement phase and rebound phase that follows that phase. The forward movement phase lasts until around t=0.5 s in the *Brake12_01* and *Brake12_02* maneuvers. In the *Brake50_01* maneuver the forward movement lasts until around t=0.4 s and was followed by a phase with constant forward excursion until around t=1.5 s. In the initial forward movement phase a qualitatively similar behavior of both head and torso movement was observed, but the magnitudes differ. *Brake50_01* lead to the smallest excursions for head and torso. Median values of both, *Brake12_02* and *Brake50_01* are comparable in the initial phase of the movement, while *Brake12_01* lead to larger median and upper corridor limit curves in both body segments.

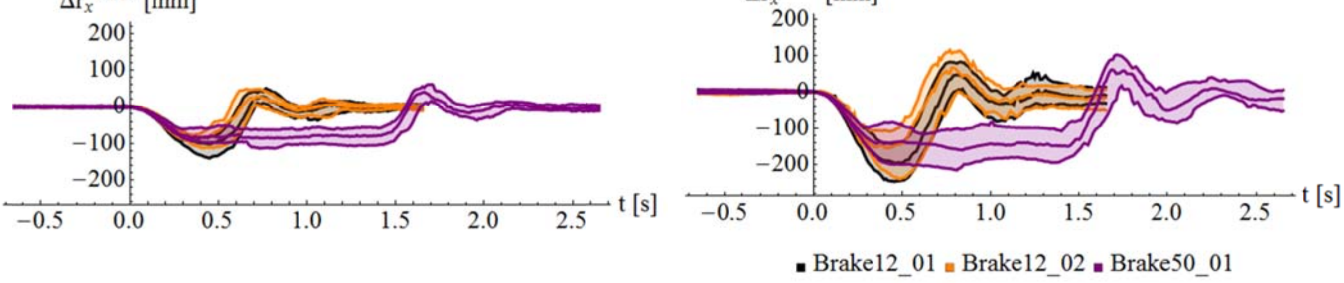

Fig. 4: Corridors for the centroid displacement time history in frontal direction Δr_x of torso (left) and head (right) for emergency braking maneuvers.

Although there was negligible lateral motion the torso showed a rotation around the z-axis of up to 12° (median), peaking at around t=0.45 s. No such pattern can be observed in the head rotation around the same axis, but rotations with a magnitude of 4° in both directions occurred in this phase. In Fig. 5 corridors of torso and head segment orientation around the z-axis $\phi^{Torso}{}_z$ and $\phi^{Head}{}_z$ are displayed. A significant torso segment orientation $\phi^{Torso}{}_z$ was observed in all three maneuvers for the forward and backward movement indicating a pure rotation of the torso, while the head kept its orientation. The rotation was such that the left shoulder shows further excursion than the right shoulder, which was consistent with the subject being held back by the upper leg of the three-point belt

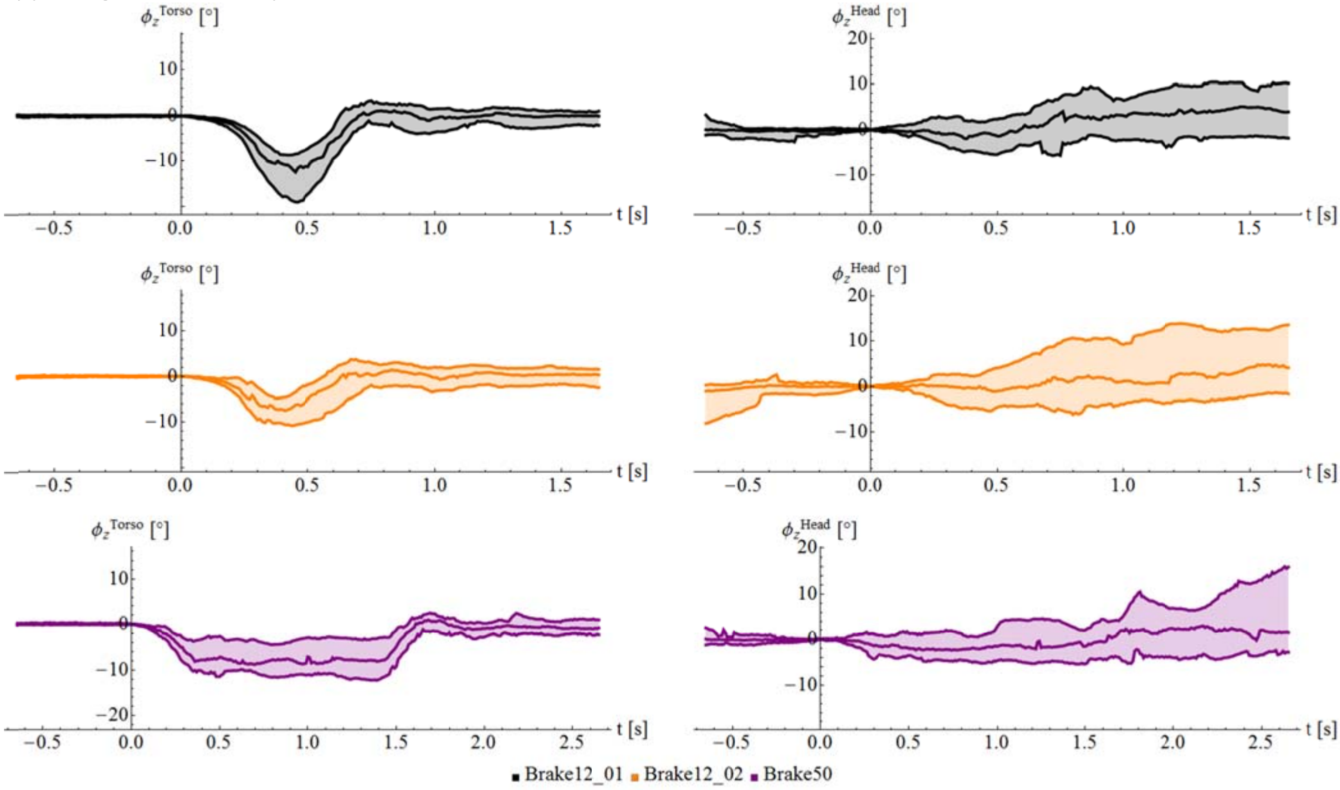

Fig. 5: Corridors of the torso segment orientation around the z-axis ϕ_z^{Torso} (left and the orientation of the head ϕ_z^{Head} (right) for three emergency braking maneuvers.

The orientation of the torso segment, which was determined from markers on the thorax and shoulder girdle, is a result from various rotations along the spine. In Fig. 6 the angle that corresponds to the forward excursion of the torso segment around the y-axis ($\Phi^{Torso}{}_y$) is compared to the orientation of the segment around the same axis and also the difference thereof is displayed. Since $\Phi^{Torso}{}_y$ is larger than -$\phi^{Torso}{}_y$ (*Brake12_02*: peak median differences of 2°, *Brake12_01* and *Brake50_01:* 4° in the initial forward movement and the plateau phase of the maneuver) this indicates an effective flection in the lumbar spine area.

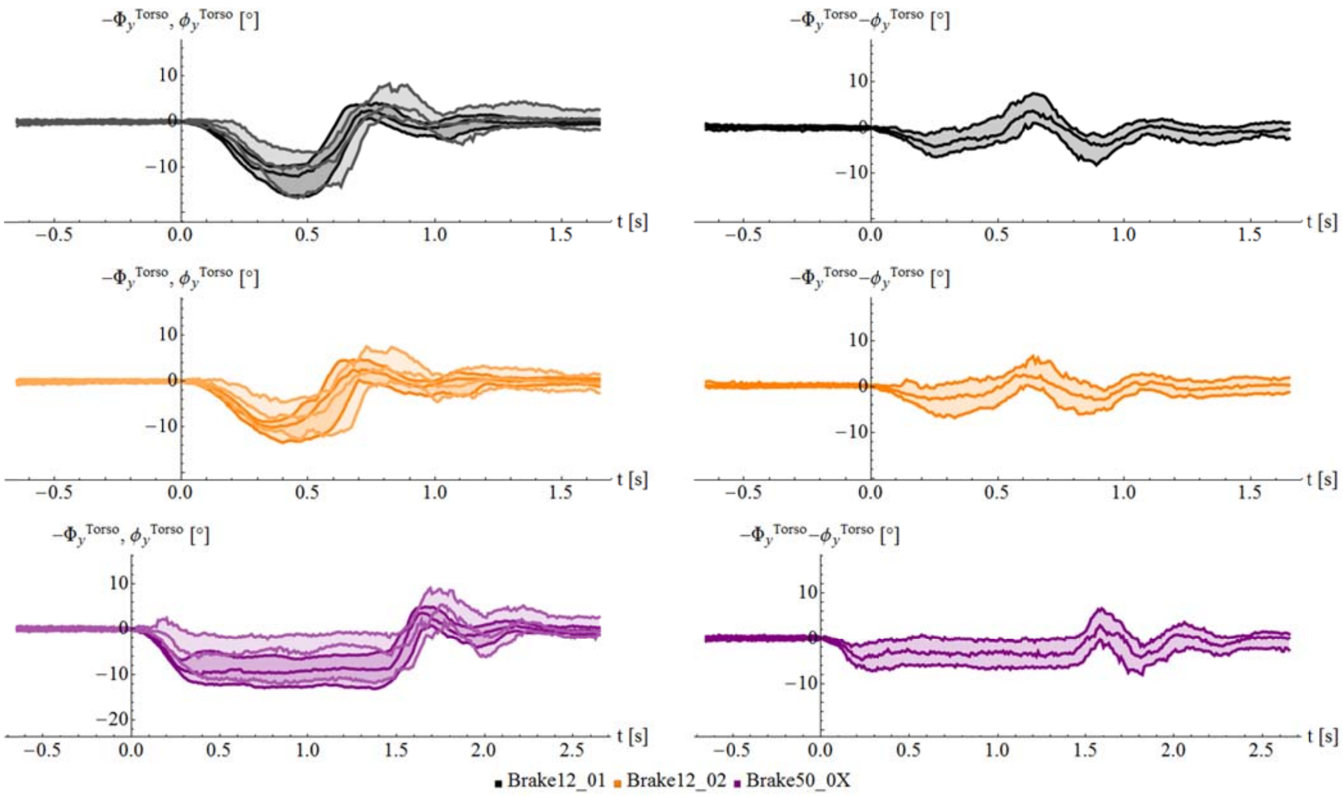

Fig. 6: Corridors of the torso centroid angle Φ_y^{Torso} (left, darker lines and filling), the segment orientation ϕ_y^{Torso} (left, lighter lines and filling) and the difference between the two angles (right) for three emergency braking maneuvers.

B. Lane change

Lane change maneuvers were performed with an initial velocity of 50 km/h to the left and to the right, referred to as *LaneLeft50* and *LaneRight50*, respectively. Corridors for the steering wheel angle and lateral acceleration are displayed in Fig. 7. A time delay of around 130 ms between the two quantities was observed, which was also observed in [15]. Some additional quantities are presented in Fig. 19.

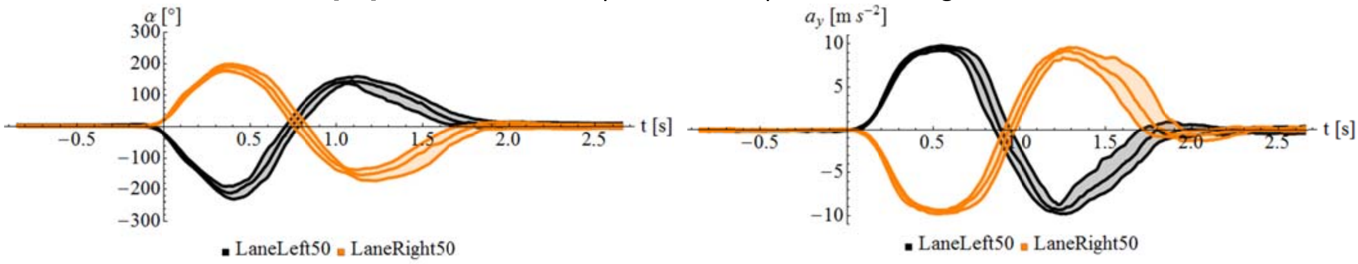

Fig. 7: Corridors including curves for the median as well as the 0.16th and 0.84th quantile of steering wheel angle α and lateral acceleration a_y are displayed vs. time for lane change maneuvers to the left and right. Note that there is a time delay of around 130 ms between onset of the steering wheel movement and lateral acceleration.

As in the previous maneuvers the main contribution to the occupant movement follows the direction of the acceleration vector, i.e. the excursions in the horizontal plane are dominant, therefore displacements of torso and head segments are displayed in Fig. 8 while the full kinematic results are collected in the appendix (Fig. 20-Fig. 23). In order to allow for an easier comparison between the maneuver displacement values of *LaneLeft50* are inverted in Fig. 8. For the torso segment both median and upper limit curves show similar characteristics and peak excursion in the initial sideward movement. For both the lower corridor limit in the initial phase and the backwards movement there were however some differences between the maneuvers. The head segment showed larger excursions in the initial movement phase in the *LaneRight50* maneuver. In this maneuver the initial movement of the subject was towards the center of the vehicle, while in *LaneLeft50* the subject moved towards the door. This result is consistent with a protective movement to avoid too close proximity to the Bpillar. Comparing the peak head excursion in the first phase of the movement in a one-factor ANOVA however reveals that there is no significant difference ($F(1,40)=2.668$, $P=0.11$).

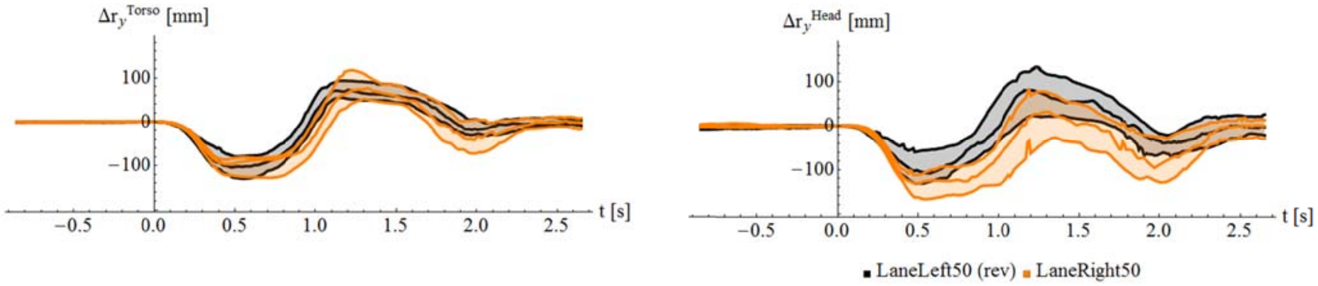

Fig. 8: Corridors for the centroid displacement time history in lateral direction Δr_y of torso (left) and head (right) for lane change maneuvers. Note that for the sake of better comparison the inverse excursions in the maneuver *LaneLeft50* are displayed.

Analogously to the emergency braking maneuvers the segment orientation ϕ_x and rotation of the torso centroid Φ_x were compared for the torso. In Fig. 9, Φ_x and the difference of the two quantities are displayed. While median values of 12° for Φ_x were observed in the first second of the maneuver only 6° thereof were accounted for by the torso orientation ϕ_x, which is consistent with a sheering movement in the torso segment.

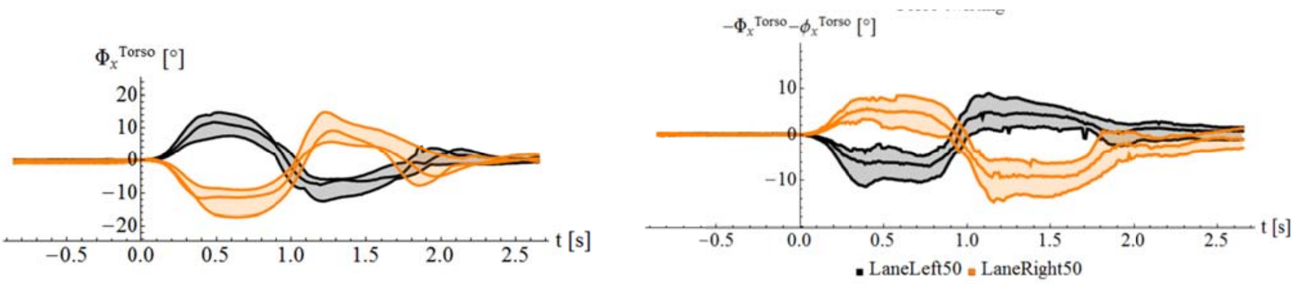

Fig. 9: Corridors of the centroid angle for the torso around the x-axis Φ_x^{Torso} (left) and the difference between centroid angle and the segment orientation around the same axis (right).

C. Combined maneuver

Two combined maneuvers with an initial velocity of 50 km/h, referred to as *CombinedRight50* and *CombinedLeft50* were performed, where the driver initiated the steering motion simultaneously with the brake pedal activation. The resulting frontal and lateral acceleration corridors are shown in Fig. 10, again with a more comprehensive collection in Fig. 24.

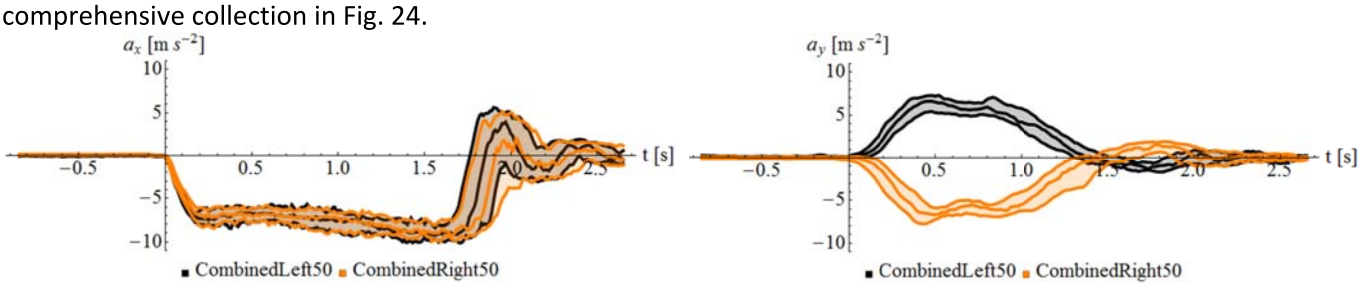

Fig. 10: Corridors of frontal and lateral acceleration a_x and a_y for combined maneuvers.

For these maneuvers more complex motions were observed and can no longer be described in a single plane. The full set of occupant kinematics was collected in the appendix (Fig. 25- Fig. 28) and excursions of head and torso segment in lateral and frontal direction are displayed in Fig. 11, where in the latter figure again the inverse lateral excursions for *CombinedLeft50* are plotted for better comparison.

Analogously to *Brake50_01* the combined maneuvers can be described in three phases. The initial forward movement lasts from t=0 to around t=0.3 s and is followed by an almost constant excursion of the head and torso until t=1.8 s. The rebound phase follows thereafter and coincides with a decreasing vehicle frontal acceleration and complete stop of the vehicle. The lateral excursion follows the same initial pattern, but the plateau-like phase only lasts until around t=1.0 s. Thereafter the lateral excursion decreases, i.e. at largely constant forward excursion the subjects return to a position dominated by forward movement. In various response curves a slight decrease of forward excursion is observed between t=0.3 s and t=0.5 s, which is most prominent in the head segment in *CombinedRight50*. In this maneuver also a slight increase of forward excursion over the plateau-like phase is observed. Similarly to the *LaneRight50* maneuver the *CombinedRight50* maneuver also shows larger lateral head excursions. Here a one-factor ANOVA shows a significant difference with (F(1,39)= 6.907, P=0.01), however.

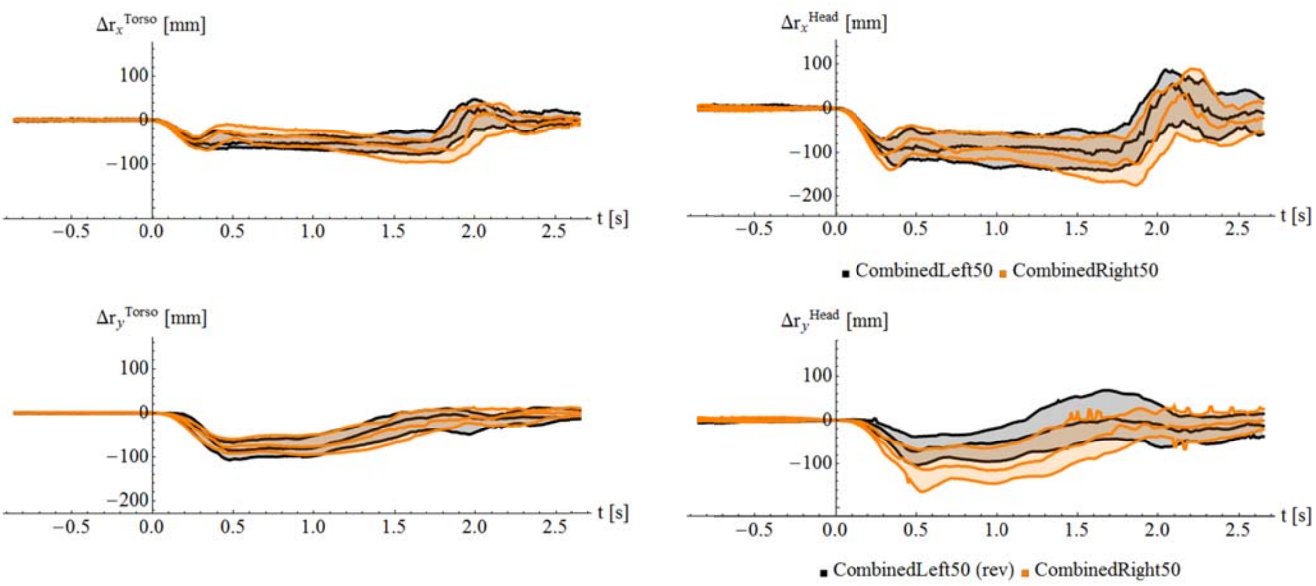

Fig. 11: Corridors for the centroid displacement time history in frontal (Δr_x, first row) and lateral direction (Δr_y, second row) of the torso (left) and head (right) for combined maneuvers. Note that for the sake of better comparison the inverse lateral excursions in the maneuver *CombinedLeft50* are displayed.

D. Load case comparison and direction of movement

In Fig. 12 maximum head and torso excursions projected to the horizontal plane are presented. As previously stated the movement during emergency braking and lane change maneuvers is predominantly observed in the frontal and lateral direction, respectively. While the torso motion in the *CombinedRight50* and *CombinedLeft50* load cases is restricted to a range comparable to that in the other maneuvers, the maximum head excursion is observed in locations compatible with braking maneuvers, i.e. predominantly excursion to the front, but also with significant lateral components, similar to what is observed in lane change maneuvers.

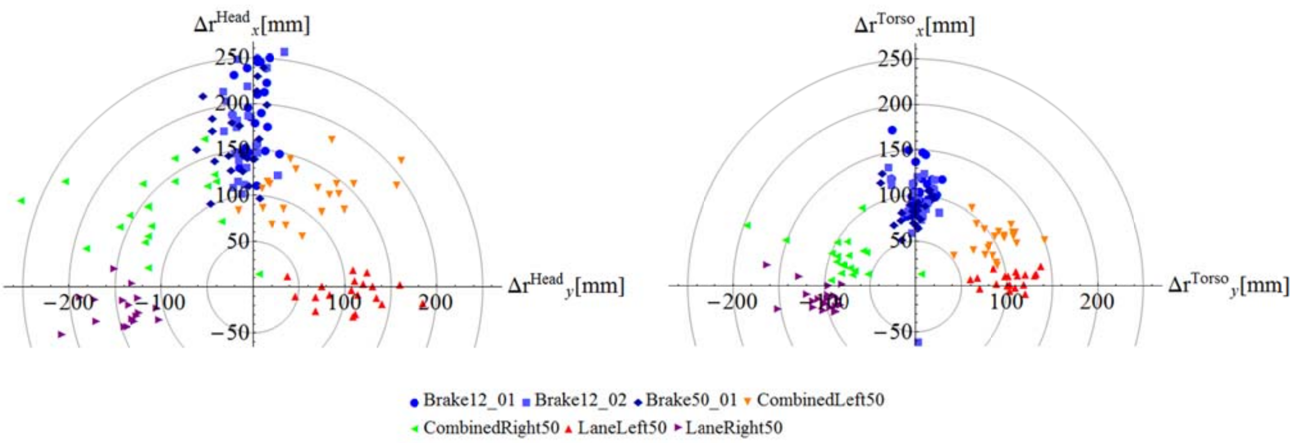

Fig. 12: Maximum excursion Δr of head and torso during various maneuvers. Note that maneuvers to the left lead to an initial movement to the right.

E. Comparison

In order to compare different maneuvers among each other the norm of the maximum head and torso excursions projected to the transverse plane are displayed in Fig. 13. All maneuvers show comparable mean torso forward movement in the region between 86 mm and 112 mm. For the head movement a tendency of larger excursions in the frontal maneuvers, especially *Brake12_01*, can be observed. The significantly smaller head excursion in the *CombinedLeft50* with respect to the *CombinedRight50* maneuver has also already been mentioned. A complete table of results can be found in Table 2.

TABLE II
MAXIMUM EXCURSIONS OF HEAD AND TORSO IN VARIOUS MANEUVERS

	Δr^{Head}_x [mm]	Δr^{Head}_y [mm]	Δr^{Head} [mm]	Δr^{Torso}_x [mm]	Δr^{Torso}_y [mm]	Δr^{Torso} [mm]
Brake12_01	-200 ±49	2 ±14	200 ±48	-111 ±22	5 ±14	112 ±23
Brake12_02	-171 ±52	-6 ±18	172 ±52	-88 ±36	2 ±14	94 ±20
Brake50_01	-158 ±40	-15 ±23	161 ±40	-85 ±17	-2 ±15	86 ±18
LaneLeft50	6 ±15	107 ±37	109 ±37	-7 ±9	104 ±22	105 ±22
LaneRight50	35 ±31	-123 ±72	146 ±30	13 ±14	-103 ±22	105 ±22
CombinedLeft50	-103 ±26	62 ±47	126 ±39	-51 ±15	89 ±22	104 ±21
CombinedRight50	-86 ±39	-105 ±62	145 ±52	-33 ±20	-79 ±37	88 ±36

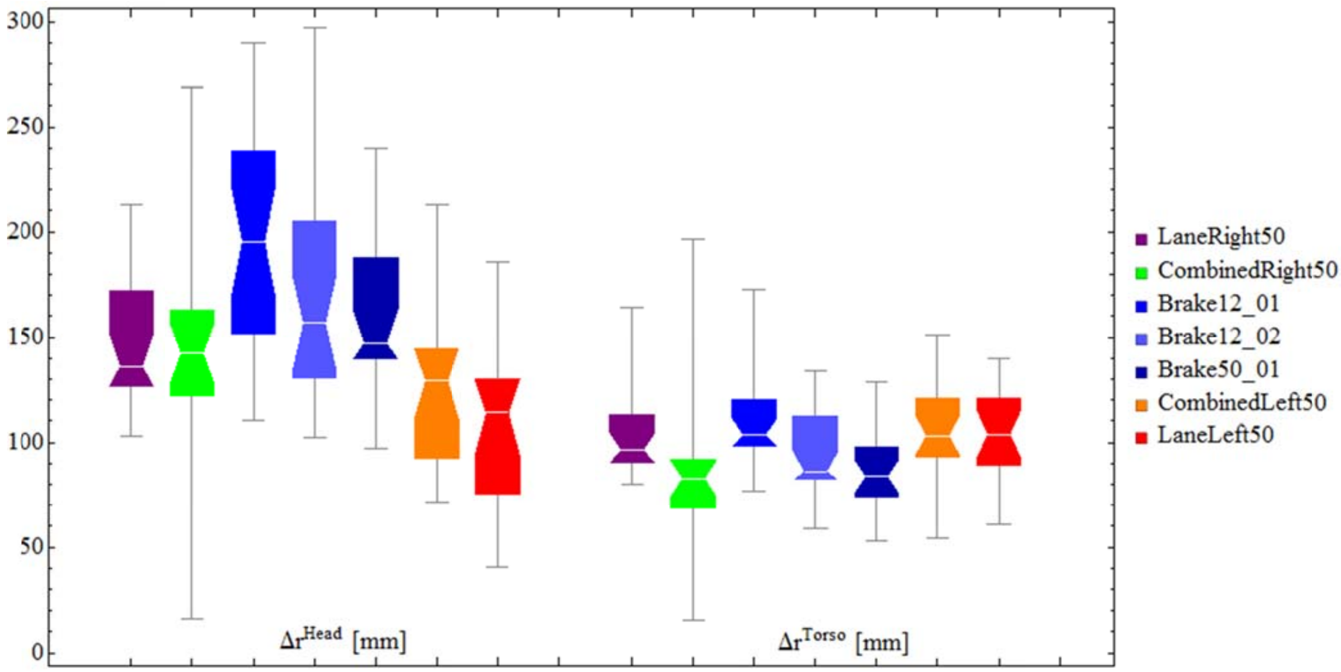

Fig. 13: Centroid displacement Δr for the head (left) and torso (right) segment projected to the transverse plane for all seven types of maneuvers. The error bars indicate the range of values within a set, the boxes denote the region between the 25th and the 75th percentile with the central white line marking the median value.

Each subject was exposed to each maneuver. In order to discuss the between-subject variability and between-maneuver variability all absolute head and torso excursion values were scaled by their respective group mean and standard deviation using

$$z_{\text{Segment,Maneuver}} = \frac{\Delta r_{\text{Segment,Maneuver,Subject}} - \mu_{\text{Segment,Maneuver}}}{\sigma_{\text{Segment,Maneuver}}}. \quad (1)$$

Two limiting cases were also considered, one being a strict correlation of excursion to the subjects, which was created by sorting all z-values by magnitude and grouping them to sets of the appropriate size to match the maneuver number for each subject, a case where the within-subject variability is minimized and the majority of variation is due to having different types of subjects (e.g. slack and tense) in the test population. The second limiting case was derived by randomly resampling the z-values and again grouping them to sets of the appropriate size. For the latter case a corridor for the mean values was computed from several resampling operations. This corresponds to a situation where no clear ordering of subject types is possible.

These limiting cases together with the actual z-values are displayed in Fig. 14, where all subgroups are sorted according to their group median value. For both cases the observed distribution of rescaled excursions lie between the two limiting cases, indicating a possible distinction of response types.

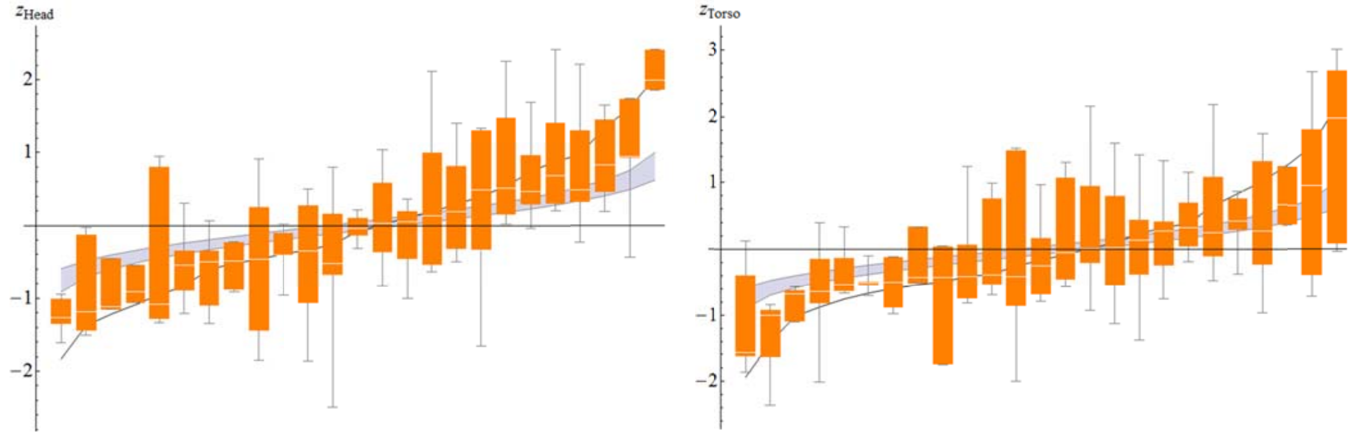

Fig. 14: Rescaled values of the torso (right) and head (left) excursion (boxes; for a description refer to Fig. 13) across all maneuvers sorted by the subject median. For the sake of comparison the limiting case for the within-subject mean of a strict ordering of subject excursion is displayed in black. A corridor of the estimated within-subject mean values of a random sample of rescaled excursion values is displayed in gray.

IV. DISCUSSION

Compared to the results for the braking maneuvers in [13] the average maximum head and torso excursions changed only slightly due to inclusion of a larger set of test subjects. Therefore no detailed comparison of the results to results in [7] and [12] are given here, but the reader is referred to the discussion in [13] instead.

For lane change maneuvers results changed considerably by including a larger number of subjects. Values of 104±22 mm (torso) and 107±37 mm (head) for the excursion were observed in *LaneLeft50* and -103±22 mm (torso) and -123±72 mm (head) in *LaneRight50*. In [9] lateral head excursions of 171±58 mm and 121±46 mm for relaxed and braced subjects were reported for lateral peak accelerations of 5 $m{\cdot}s^{-2}$. Although subjects in this study were not instructed to brace, the comparably small lateral head and torso excursions may be due to the lateral support structures of the modified seat.

To the authors' knowledge no detailed kinematic results for combined lateral and frontal maneuvers have been reported yet, therefore only a comparison to braking and lane change maneuvers is possible at this stage. Therefore, both the head and torso maximum excursions values comparable to braking and lane change maneuvers were observed. In contrast the associated direction of the peak excursion in the transverse plane varied considerably more in the combined maneuvers. Both observations are not surprising, since the torso movement is restricted by the upper part of the tree-point belt in braking and combined cases and the lateral support of the seat in the lane change cases. Also for the combined cases, the effective direction of acceleration changes over the course of the maneuver, which could explain the second observation. Despite the constraints, due to belt and seat, still large inter-subject variability of over 200% in all maneuvers was detected.

There are various limitations associated with the test setup as well as the analysis. Although the tests were performed in a production vehicle driving in a traffic-like environment the subjects were still in an explicit test scenario. The missing windshield, added cameras, modified seat and interior and the number of maneuvers in a relatively short time add to this. In the analysis data a large amount of kinematic data from numerous markers needs to be reduced to a few key quantities to characterize complex human movement and to compare different subjects and maneuvers among each other, which may obscure some more subtle details in the occupant motion. E.g. for characterizing the torso motion 12 markers including markers on C7, T1, T10 and sternum are used, which consequently does not allow to address bending of the thoracical spine. Also detailed spinal kinematics, especially in the lumbar area, can only be inferred from adjacent markers, because markers in this area would be occluded by body and seat and would probably be damaged during the maneuvers. Since there are no marker trajectories available in the lumbar spine and parts of the pelvis area the occupants' motion on the seat surface could not be measured. Therefore also a qualitative comparison between the original seat and the seat used in this study is not possible, which is a further limitation of the study. However from video recordings no major sliding motions were identified. Female and male subjects were tested with a large range of different anthropometric properties. Nevertheless no analysis concerning these influence factors is presented here, which remains work to be done.

The results presented in the study will provide a basis for the kinematic validation of active human body models. With the corridors provided e.g. the range of excursions that such models need to be able to simulate can be determined. Also “average”, “slack” and “tense” response types could be identified. For very detailed implementation of muscle activity and posture control as well as simulation of internal forces additional measures such as muscle activity measurements and forces exerted on belt, seat and steering wheel could be beneficial.

V. CONCLUSIONS

In this study a detailed analysis of occupant kinematics with up to 25 subjects under emergency braking, lane change and combined maneuvers is presented. Detailed vehicle and occupant kinematic corridors are also presented. Largely consistent excursion magnitudes over all maneuvers were recorded with an inter-subject variability of above 200% for every maneuver. Torso rotation due to the asymmetry of the tree-point belt were addressed in detail for emergency breaking maneuvers and left-right asymmetries in lateral excursions were addressed in the remaining maneuvers. Also a sheering motion in the torso for brake and lane change maneuvers was identified.

Results from all load-cases were combined and consistent excursion values for the torso were found across all maneuvers. Head excursions showed larger variations with the initial braking maneuver leading to the largest values and the lane change maneuver to the left, to the smallest values.

VI. ACKNOWLEDGEMENT

VIRTUAL VEHICLE Research Center is funded within the COMET – Competence Centers for Excellent Technologies – programme by the Austrian Federal Ministry for Transport, Innovation and Technology (BMVIT), the Federal Ministry of Science, Research and Economy (BMWFW), the Austrian Research Promotion Agency (FFG), the province of Styria and the Styrian Business Promotion Agency (SFG). The COMET programme is administrated by FFG.

We would, furthermore, like to express our thanks to our supporting industrial and scientific project partners, in alphabetical order: Daimler AG (DI Christian Mayer), Partnership for Dummy Technology and Biomechanics (Dr. Norbert Praxl), Volkswagen AG (DI Jens Weber, DI Emrah Yigit), Graz University of Technology, Vehicle Safety Institute, Austria.

VII. REFERENCES

[1] E. Commission, "Towards a European road safety area: policy orientations on road safety 2011-2020".

[2] "Vision Zero Initiative," [Online]. Available: http://www.visionzeroinitiative.com/.

[3] S. Ejima, K. Ono, S. Holcombe, K. Kaneoka and M. Fukushima, "A study on occupant kinematics behaviour and muscle activities during preimpact braking based on volunteer tests," in *International IRCOBI Conference on the Biomechanics of Impact*, Maastricht, The Netherlands, 2007.

[4] S. Ejima, Y. Zama, F. Satou, S. Holcombe, K. Ono, K. Kaneoka and I. Shiina, "Prediction of the Physical Motion of the Human Body based on Muscle Activity during Pre-Impact Braking," in *International IRCOBI Conference on the Biomechanics of Impact*, Bern, Switzerland, 2008.

[5] S. Ejima, D. Ito, F. Satou, K. Mikami, K. Ono, K. Kaneoka and I. Shiina, "Effects of Pre-impact Swerving/Steering on Physical Motion of the Volunteer in the Low-Speed Side-impact Sled Test," in *International IRCOBI Conference on the Biomechanics of Impact*, Dublin, Ireland, 2012.

[6] D. Ito, S. Ejima, S. Kitajima, R. Katoh, H. Ito, M. Sakane, T. Nishino, K. Nakayama, T. Ato and T. Kimura, "Occupant Kinematic Behavior and Effects of a Motorized Seatbelt on Occupant Restraint of Human Volunteers during Low Speed Frontal Impact: Mini-sled Tests with Mass Production Car Seat," in *International IRCOBI Conference on the Biomechanics of Impact, Götheborg, Sweden*, 2013.

[7] S. M. Beeman, A. R. Kemper, M. L. Madigan, C. T. Franck and S. C. Loftus, "Occupant kinematics in low-speed frontal sled tests: Human volunteers, Hybrid III ATD, and PMHS.," *Accid Anal Prev,* vol. 47, pp. 128-139, Jul 2012.

[8] A. R. Kemper, S. Beeman and S. M. Duma, "Effects of Pre-Impact Bracing on Chest Compression of Human Occupants in Low-Speed Frontal Sled Tests," in *22th International Technical Conference on the Enhanced Safety of Vehicles (ESV)*, Washington DC, USA, 2011.

[9] L. v. Rooij, H. Elrofai, M. M. G. M. Philippens and H. A. M. Daanen, "Volunteer kinematics and reaction in lateral emergency maneuver tests.," *Stapp Car Crash J,* vol. 57, pp. 313-342, Nov 2013.

[10] S. Carlsson and J. Davidsson, "Volunteer occupant kinematics during driver initiated and autonomous braking when driving in real traffic environments," in *International IRCOBI Conference on the Biomechanics of Impact*, Krakow, Poland, 2011.

[11] J. Östh, J. M. Olafsdóttir, J. Davidsson and K. Brolin, "Driver kinematic and muscle responses in braking events with standard and reversible pre-tensioned restraints: validation data for human models.," *Stapp Car Crash J,* vol. 57, pp. 1-41, Nov 2013.

[12] J. M. Ólafsdóttir, J. K. H. Östh, J. Davidsson and K. B. Brolin, "Passenger Kinematics and Muscle Responses in Autonomous Braking Events with Standard and Reversible Pre-tensioned Restraints," in *International IRCOBI Conference on the Biomechanics of Impact, Götheborg, Sweden*, 2013.

[13] S. Kirschbichler, P. Huber, A. Prüggler, T. Steidl, W. Sinz, C. Mayer and G. A. D`Addetta, "Factors influencing occupant kinematics during braking and lane change maneuvers in a passenger vehicle," in *International IRCOBI Conference on the Biomechanics of Impact, Berlin, Germany*, 2014.

[14] P. Huber, S. Kirschbichler, Prüggler A. and T. Steidl, "Three-dimensional occupant kinematics during frontal, lateral and combined emergency maneuvers," in *International IRCOBI Conference on the Biomechanics of Impact, Berlin, Germany*, 2014.

[15] P. Huber, M. Christova, G. A. D'Addetta, E. Gallasch, S. Kirschbichler, C. Mayer, A. Prüggler, A. Rieser, W. Sinz and D. Wallner, "Muscle activation onset latencies and amplitudes during lane change in a full vehicle test," in *Proceedings of the IRCOBI Conference*, *Götheborg, Sweden*,2013.

[16] P. Huber, C. Cagran and W. Müller, "An algorithm to correct for camera vibrations in optical motion tracking systems.," *J Biomech,* vol. 44, no. 11, pp. 2172-2176.

VIII. APPENDIX

A. Occupant response Brake12_01, Brake12_02 and Brake50_01

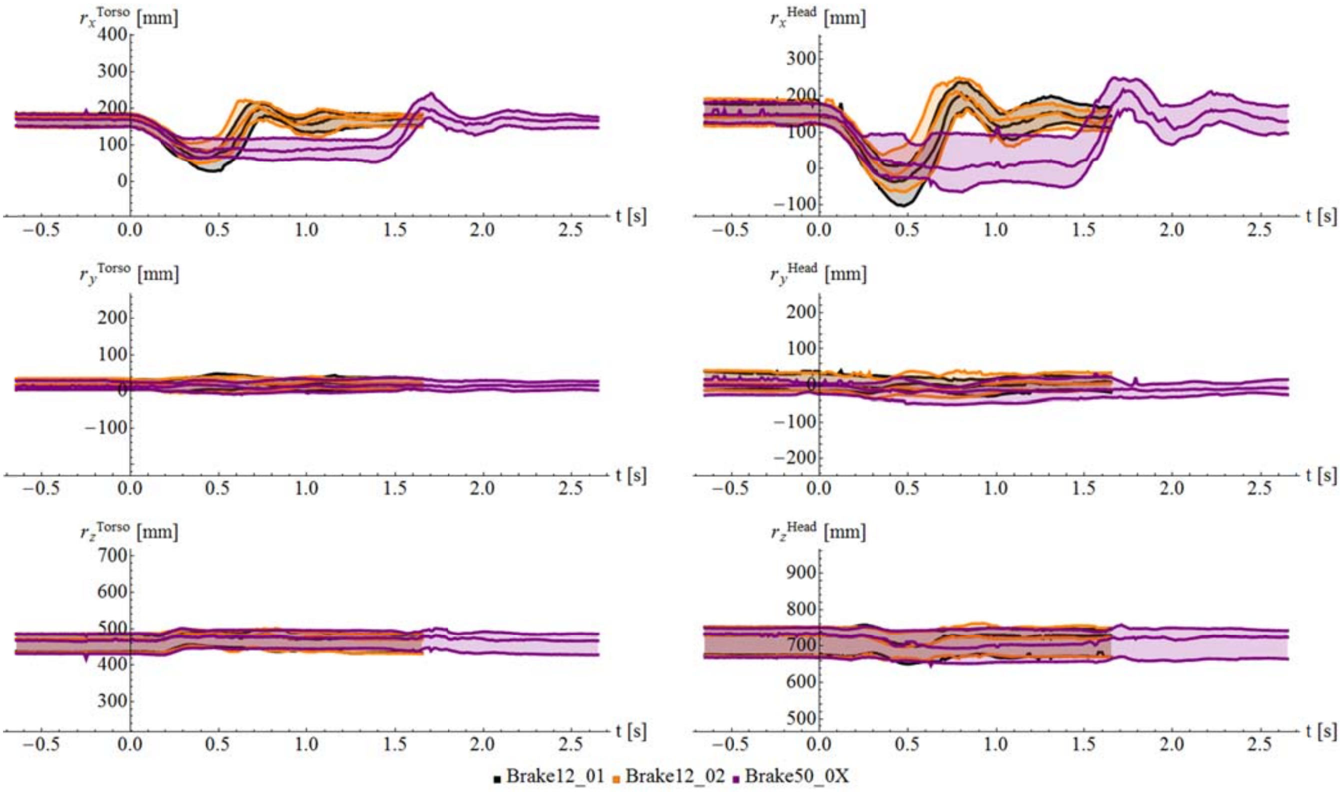

Fig. 15: Corridors for the centroid location r time history of the torso (left) and head (right) for three emergency braking maneuvers.

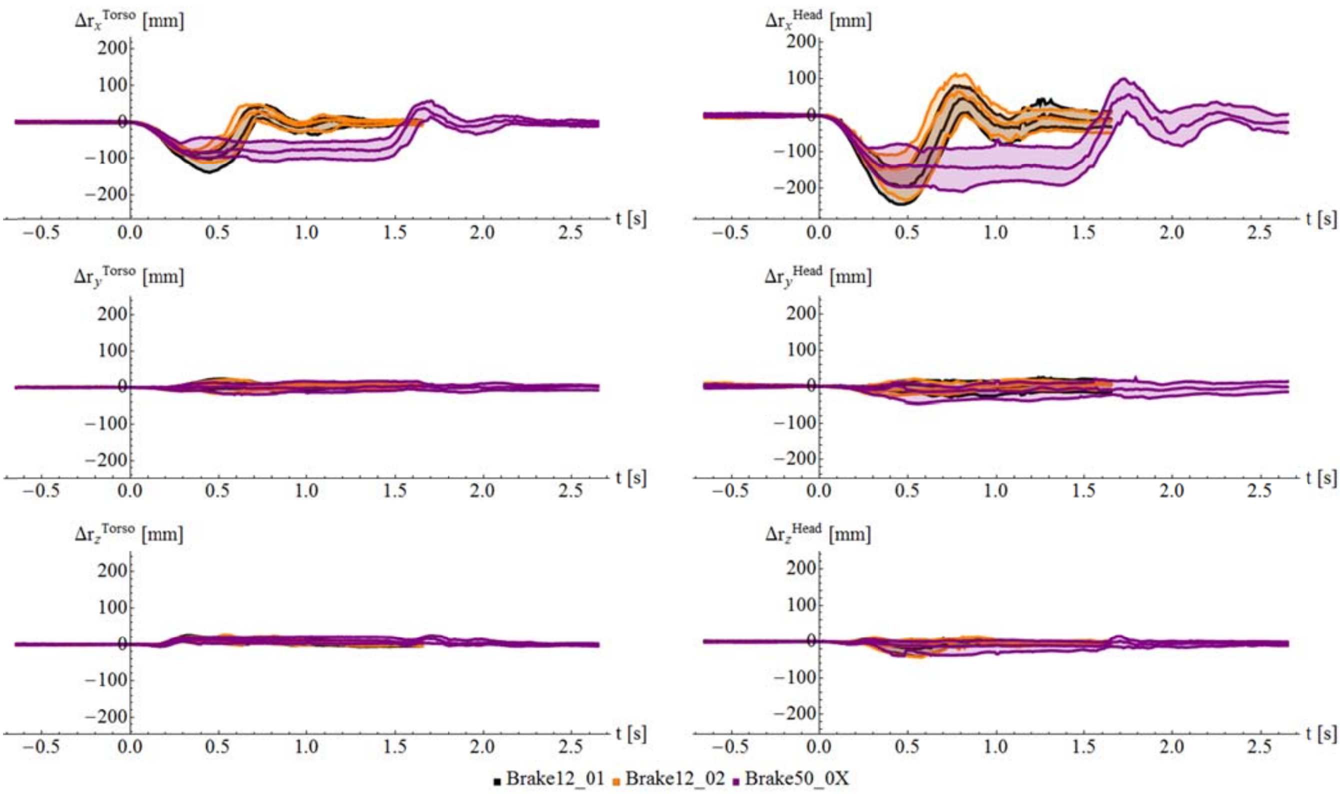

Fig. 16: Corridors for the centroid displacement Δr time history of the torso (left) and head (right) for three emergency braking maneuvers.

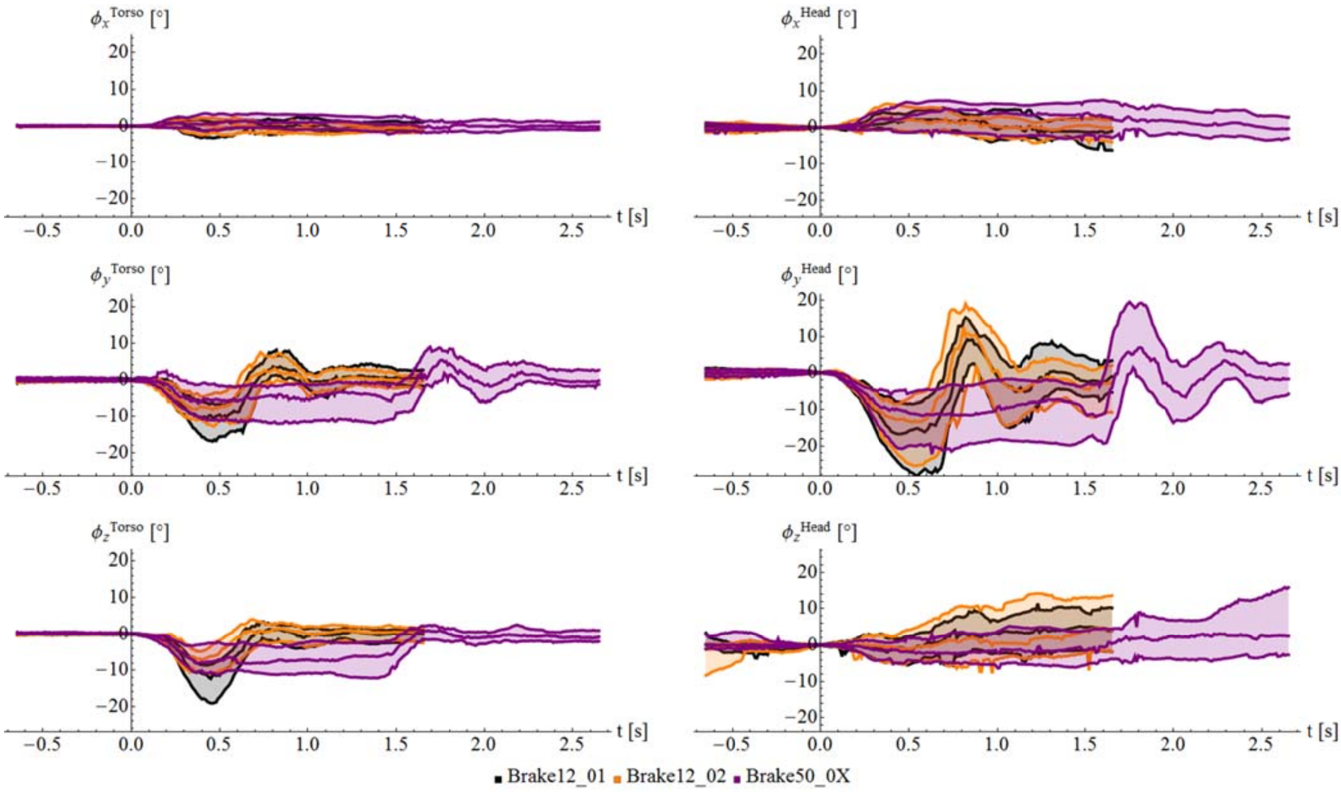

Fig. 17: Corridors for the segment orientation ϕ time history of the torso (left) and head (right) for three emergency braking maneuvers.

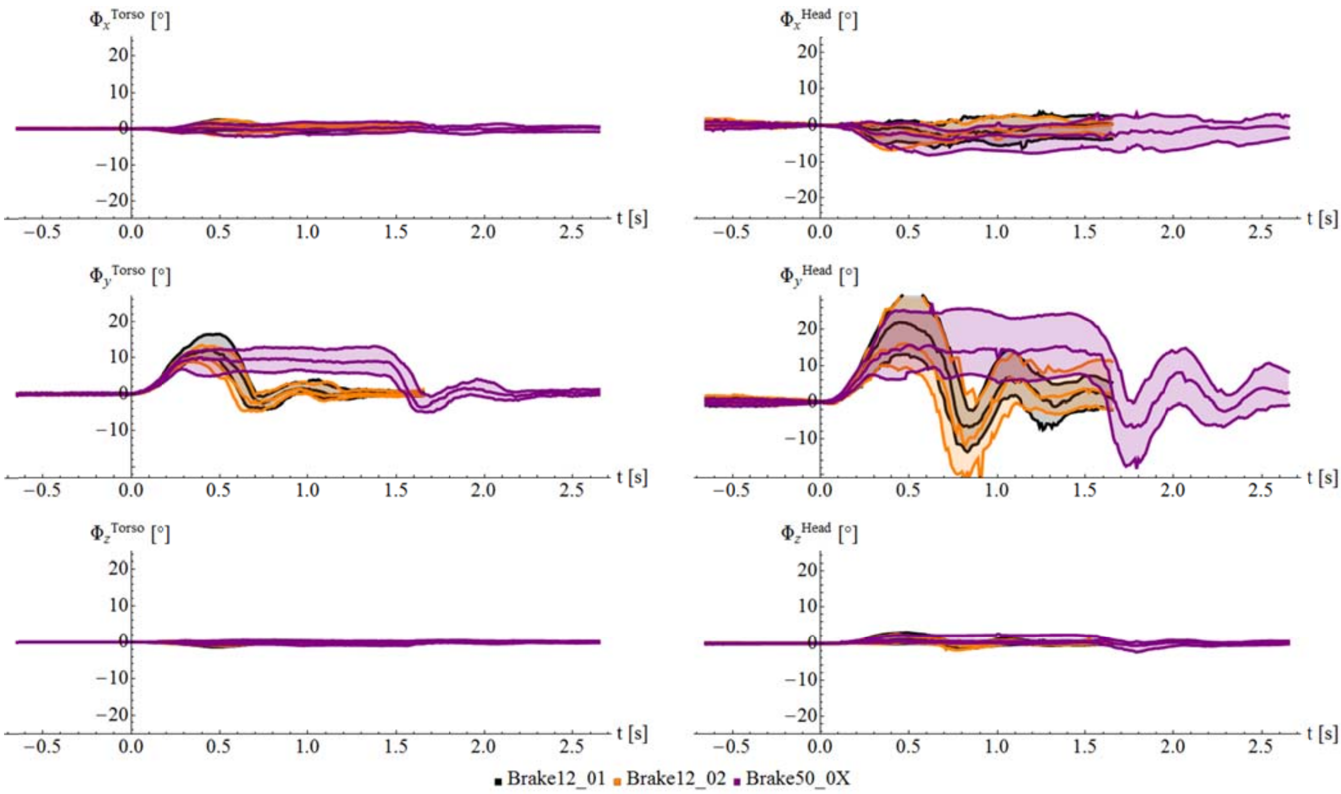

Fig. 18: Corridors for the centroid angle Φ time history of the torso (left) and head (right) for three emergency braking maneuvers.

B. Vehicle Kinematics LaneLeft50 and LaneRight50

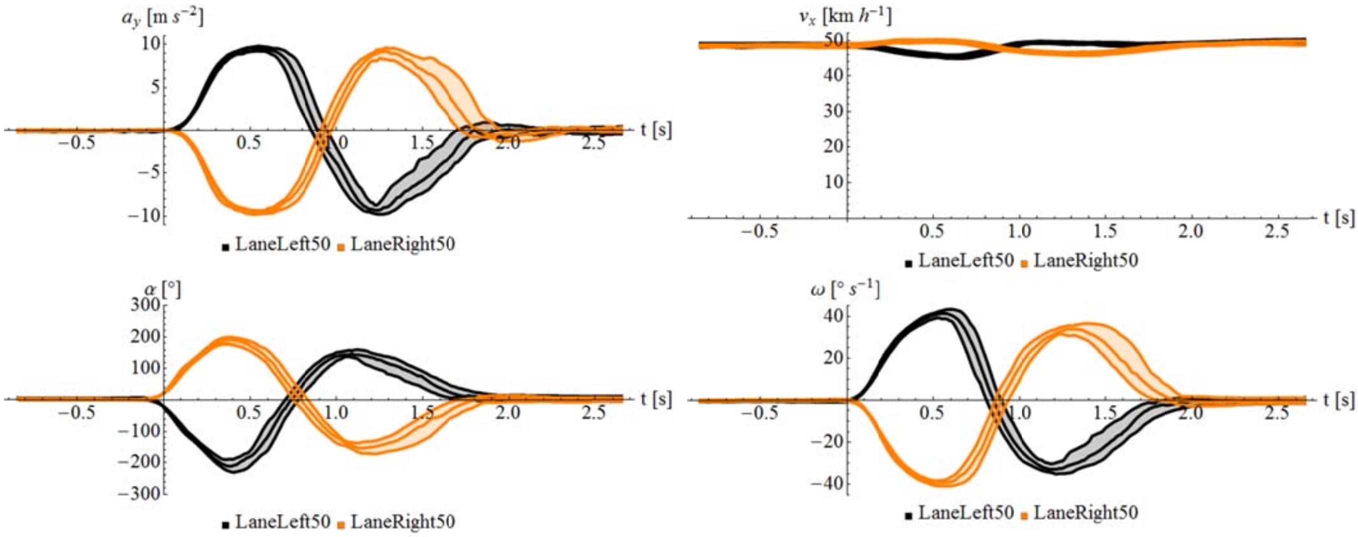

Fig. 19: Corridors of lateral acceleration a_y and velocity v_x (first row) and steering wheel angle α and yaw rate ω (last row) for lane change maneuvers.

C. Occupant response LaneLeft50 and LaneRight50

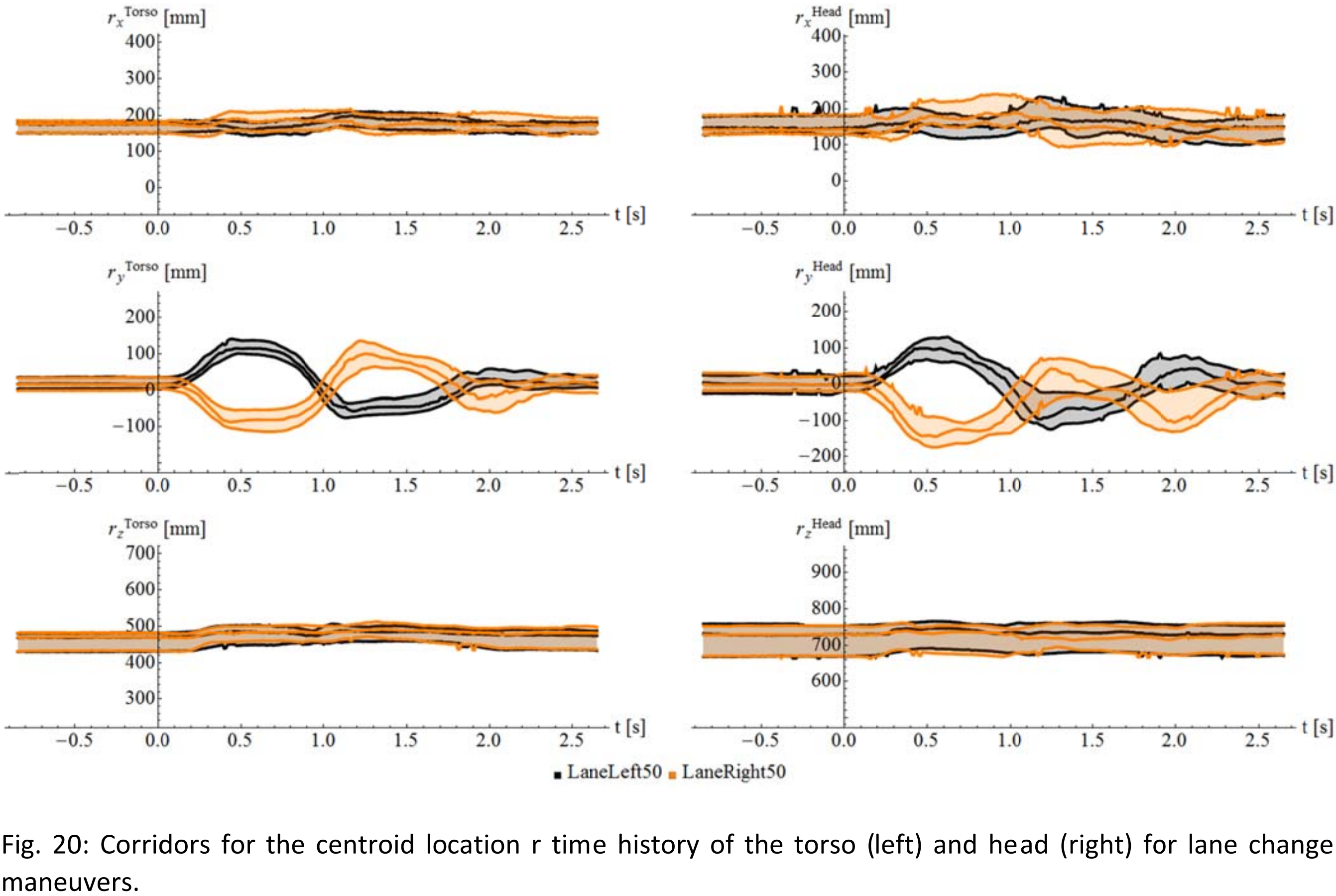

Fig. 20: Corridors for the centroid location r time history of the torso (left) and head (right) for lane change maneuvers.

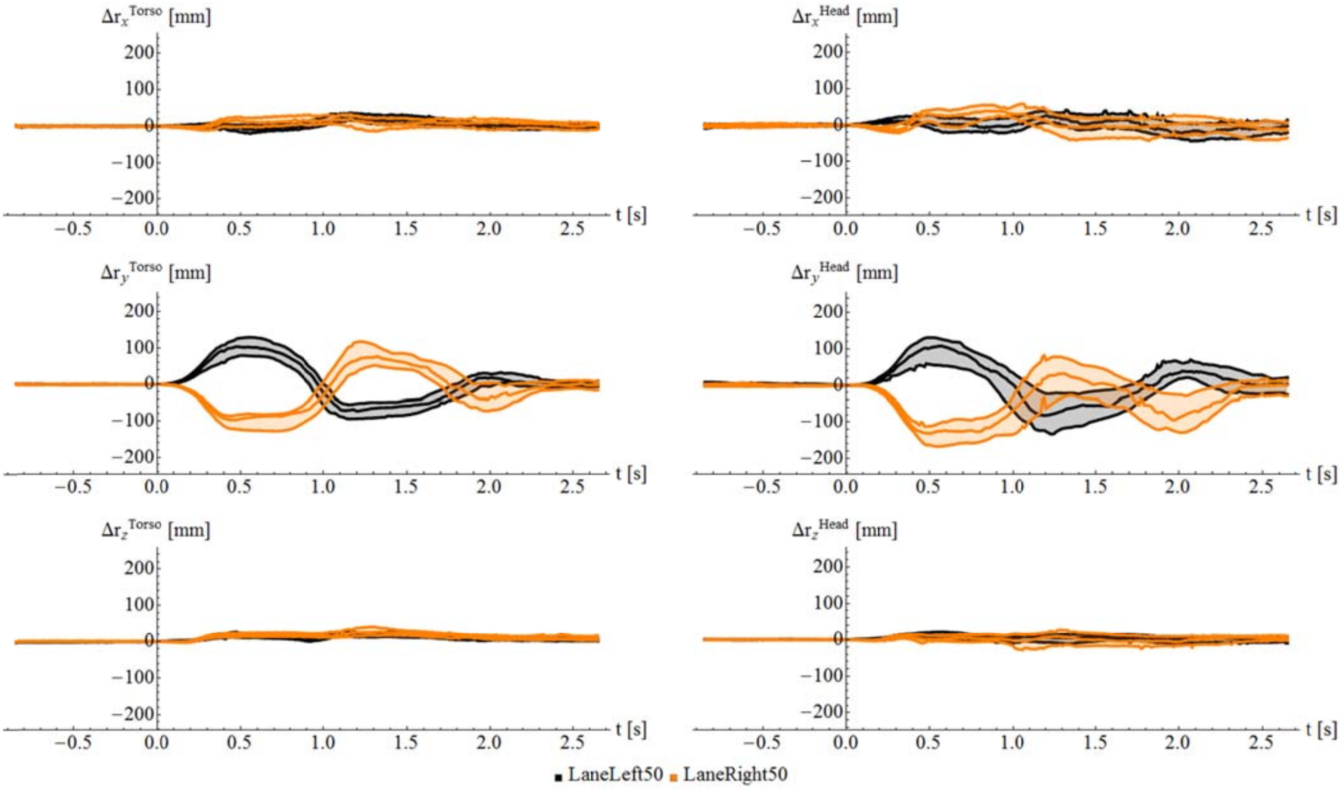

Fig. 21: Corridors for the centroid displacement Δr time history of the torso (left) and head (right) for lane change maneuvers.

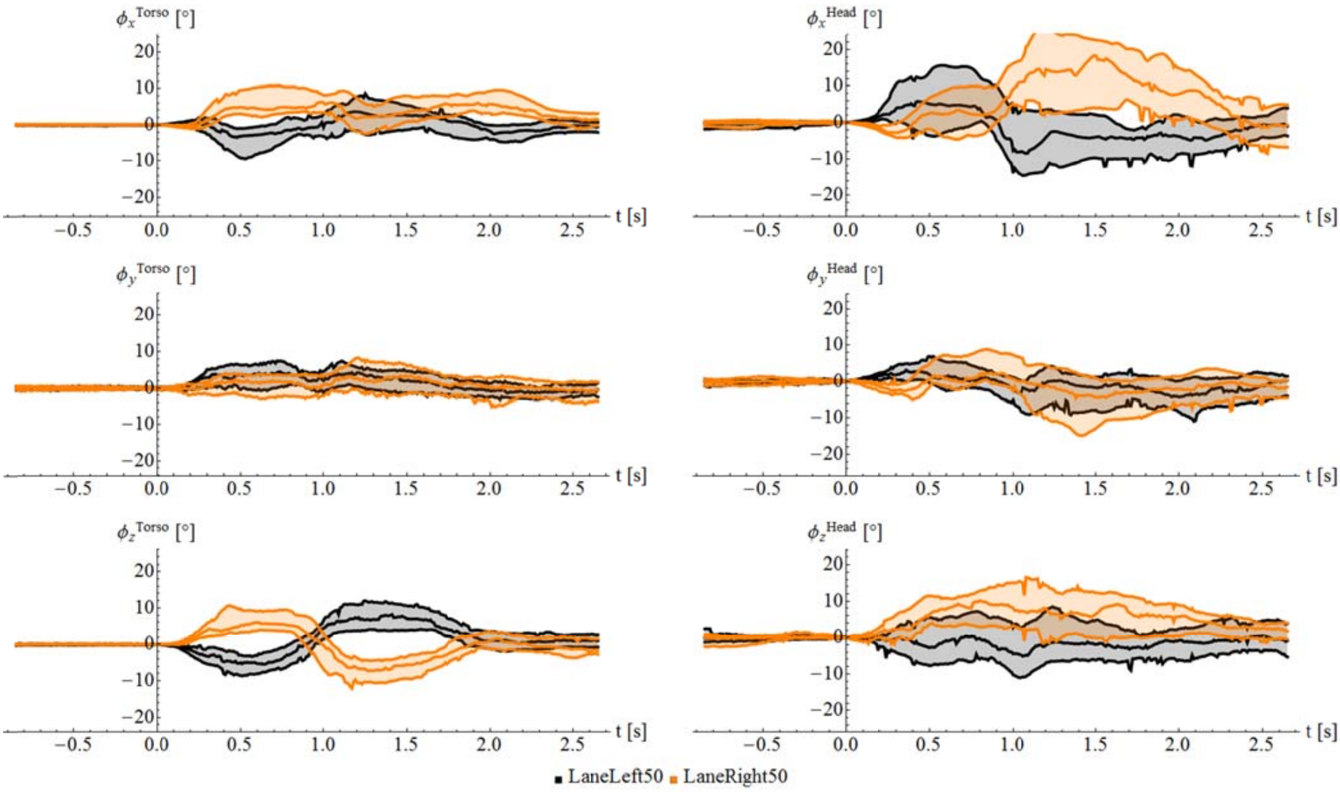

Fig. 22: Corridors for the segment orientation ϕ time history of the torso (left) and head (right) for lane change maneuvers.

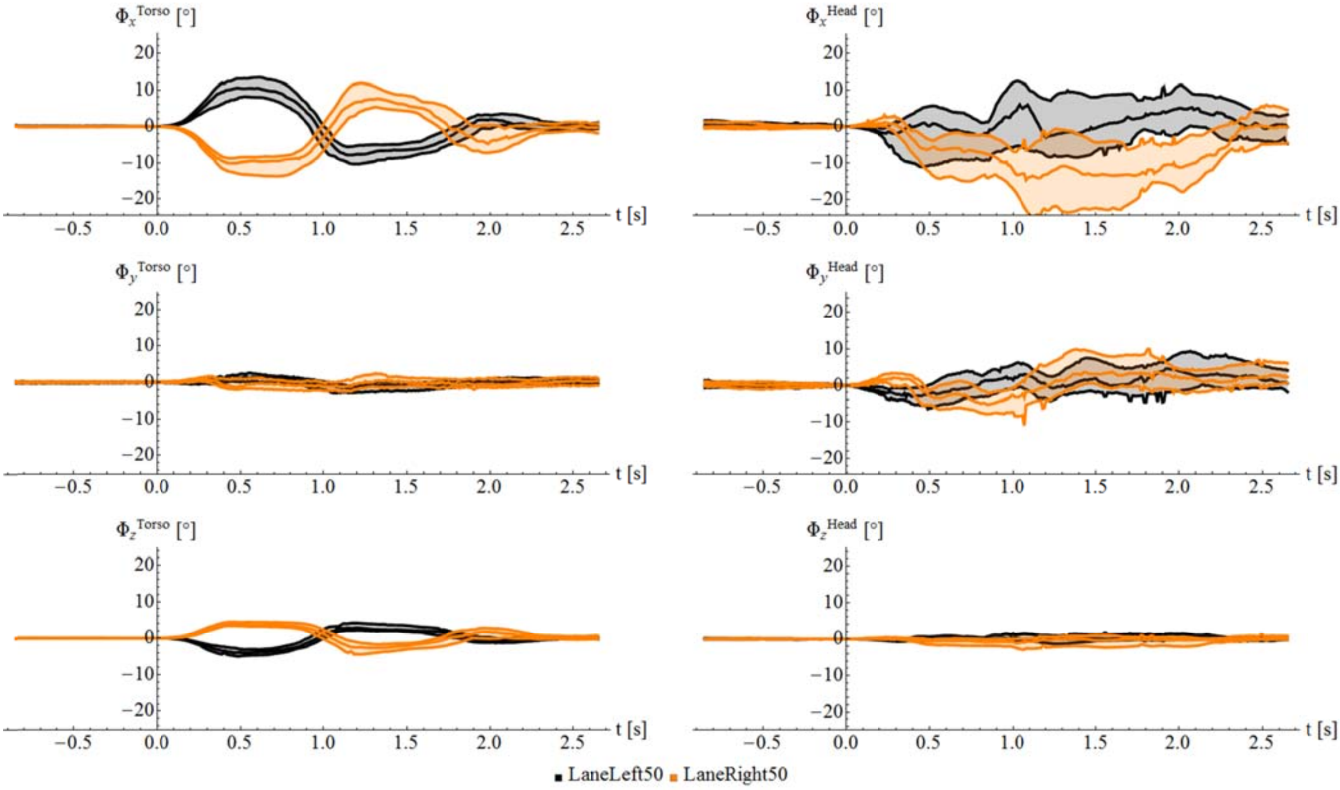

Fig. 23: Corridors for the centroid angle Φ time history of the torso (left) and head (right) for lane change maneuvers.

D. Vehicle Kinematics CombinedLeft50 and CombinedRight50

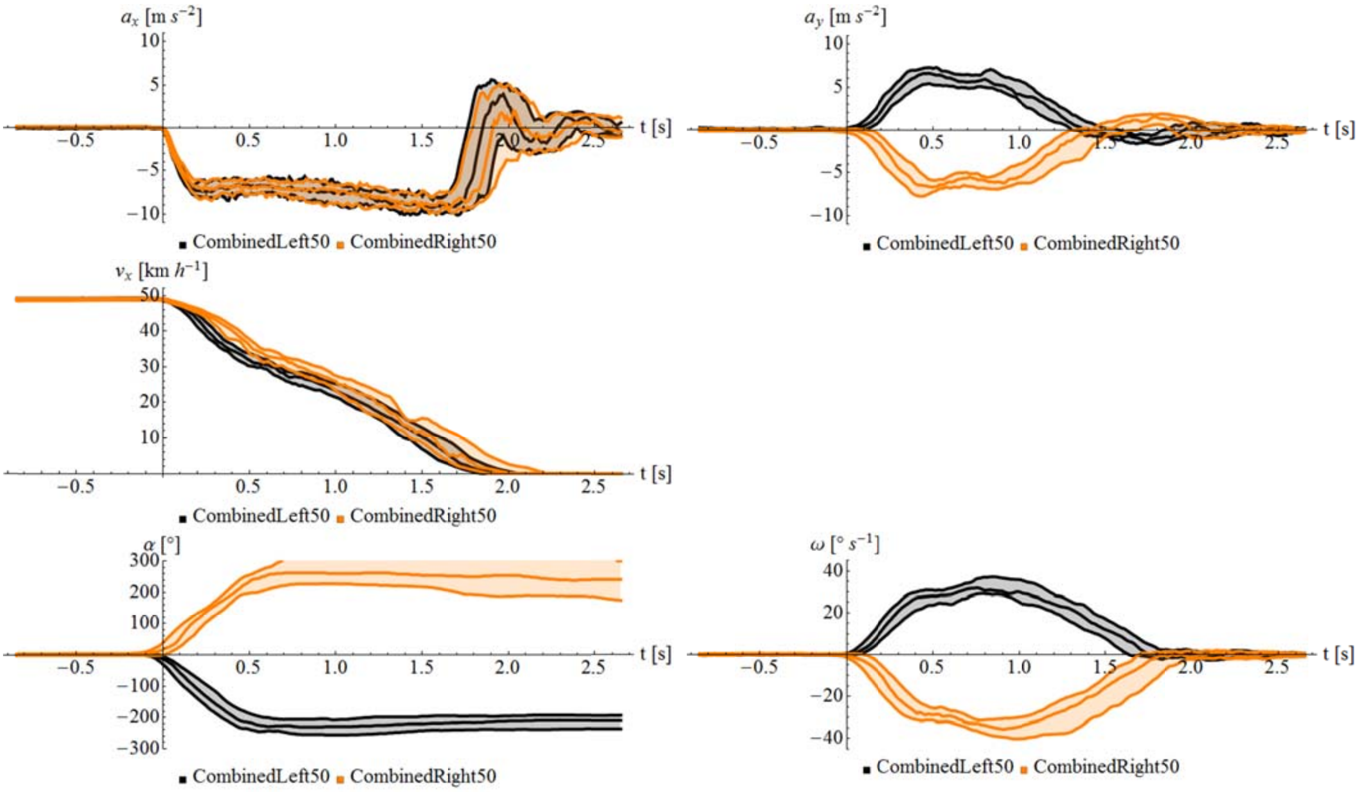

Fig. 24: Corridors of frontal and lateral acceleration a_x and a_y (first row), velocity v_x (second row) and steering wheel angle α and yaw rate ω (last row) for combined maneuvers.

E. Occupant response CombinedLeft50 and CombinedRight50

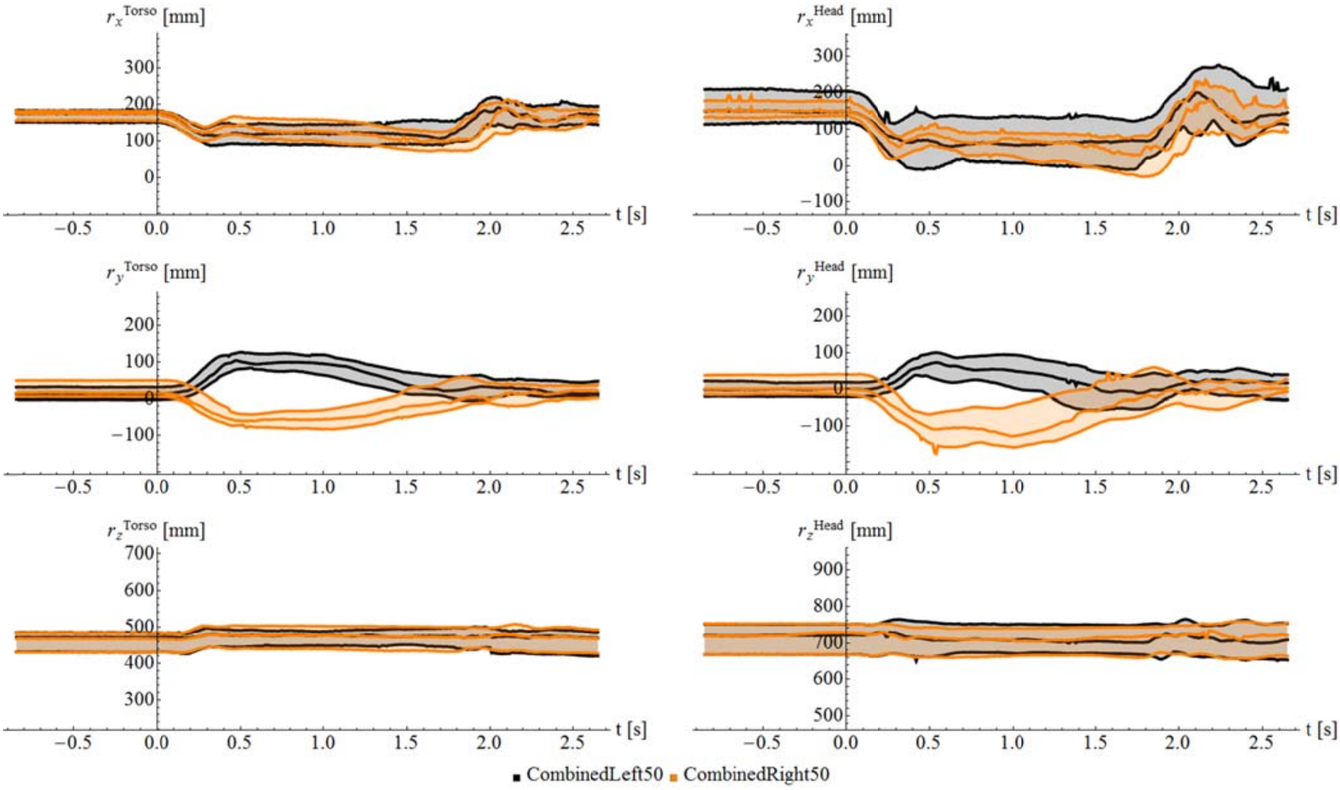

Fig. 25: Corridors for the centroid location r time history of torso (left) and head (right) for combined maneuvers.

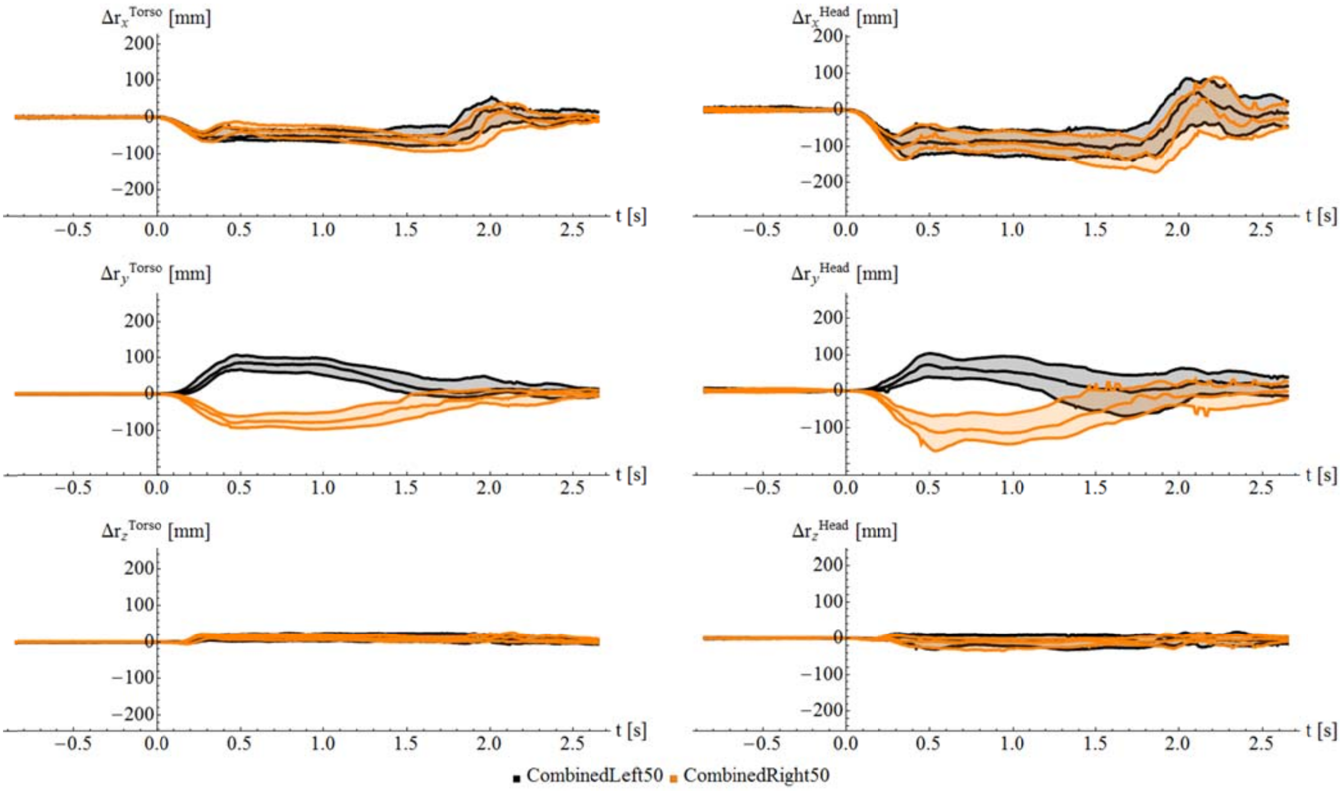

Fig. 26: Corridors for the centroid displacement Δr time history of the torso (left) and head (right) for combined maneuvers.

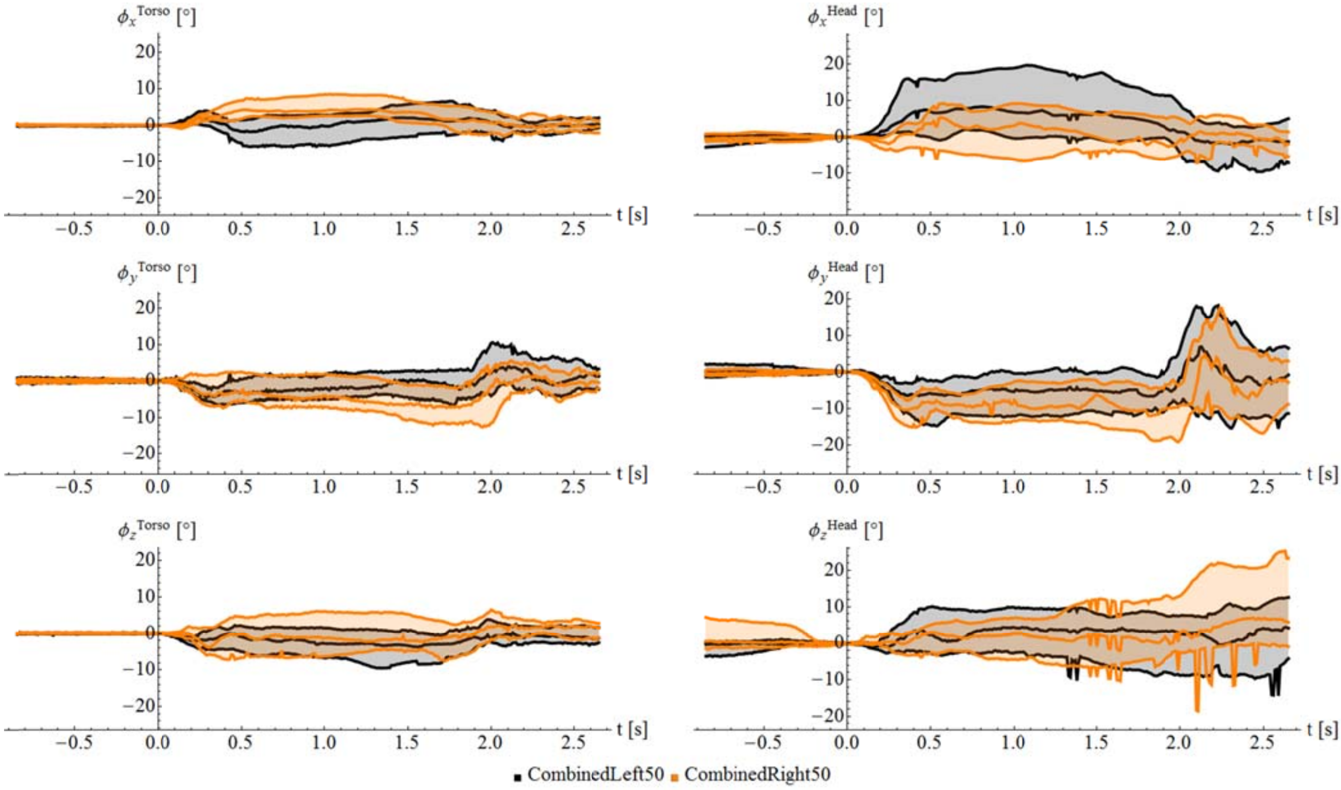

Fig. 27: Corridors for the segment orientation ϕ time history of the torso (left) and head (right) for combined maneuvers.

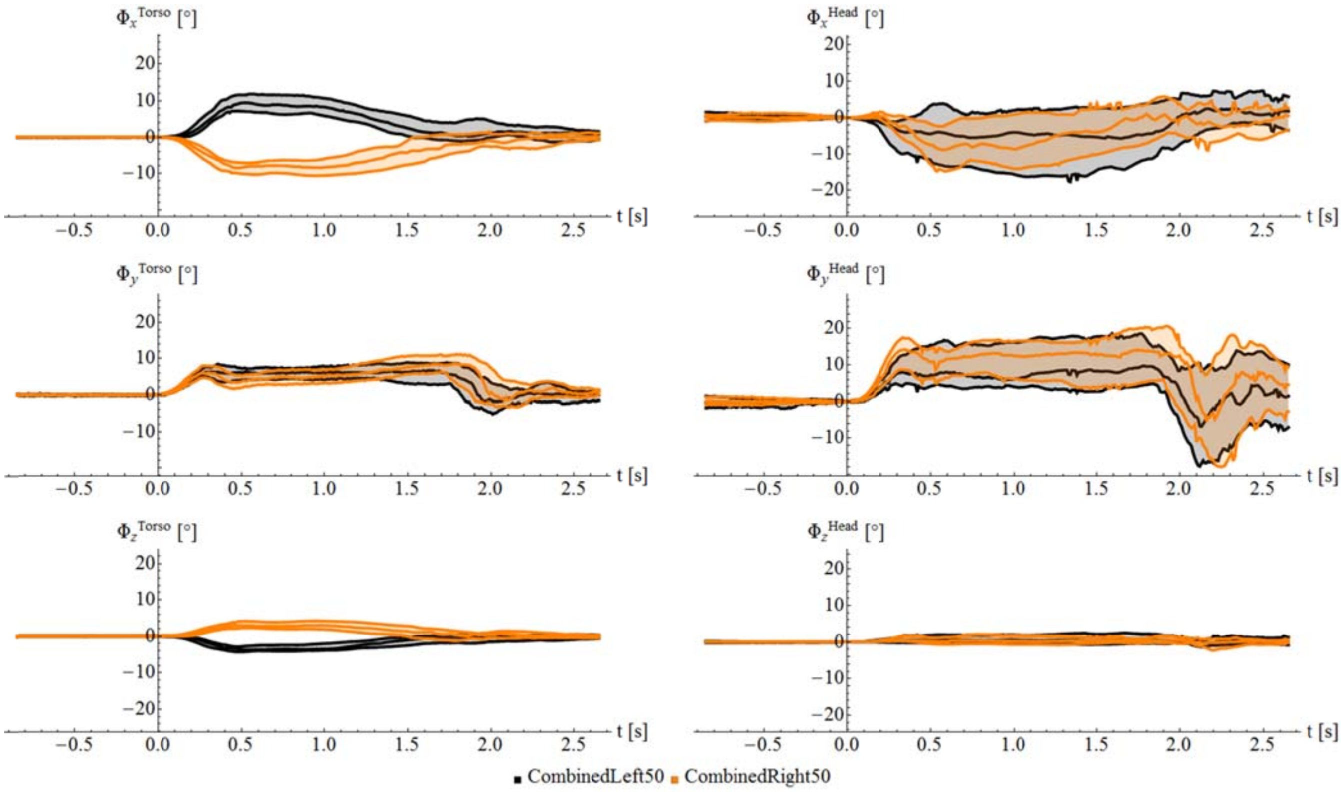

Fig. 28: Corridors for the centroid angle Φ time history of the torso (left) and head (right) for combined maneuvers.